A Two-Factor Cointegrated Commodity Price Model with an Application to Spread Option Pricing*

Walter Farkas [°‖§] Elise Gourier [°**] Robert Huitema [°] Ciprian Necula [°‡‡]

January 15, 2015

Abstract

We introduce a flexible continuous-time model of cointegrated commodity prices, which allows capturing between one and $n-1$ cointegration relations between the n components of a system. Closed-form expressions for futures and European option prices are derived. The model is estimated using futures prices of ten commodities. We find compelling evidence of multiple cointegration relationships. We calculate the prices of options written on various spreads such as the spark spread and the crack spread. We show that cointegration creates an upward sloping term structure of correlation, which lowers the volatility of spreads and consequently the price of options on them.

Keywords: Commodities, Cointegration, Futures, Option Pricing, Spread Options, Spark Spread, Crack Spread

JEL classification: C61, G11, G12

*We thank the staff from the trading and risk management divisions of AXPO AG for useful discussions and sharing data.

°University of Zurich, Department of Banking and Finance, Plattenstrasse 14, 8032 Zurich, Switzerland

‖ETH Zurich, Department of Mathematics, Rämistrasse 101, 8092 Zurich, Switzerland

§Corresponding author, Email: walter.farkas@bf.uzh.ch

**Princeton University, ORFE, Princeton, USA

‡‡Bucharest University of Economic Studies, Department of Money and Banking, Bucharest, Romania

One of the most distinctive features of commodity markets is the large number of long-run equilibrium relationships that exist between certain commodity prices. For example, the price of crude oil may move against the price of heating oil on a given day but not in the long run. That is in the long-run, the price of crude oil is tied to the price of heating oil in an equilibrium relation. These long-run equilibrium relations are usually referred to as *cointegration* relations. Cointegrated systems set in discrete time are widely employed in economics, especially empirical macroeconomics, to analyze various phenomena. Engle and Granger (1987) and Johansen (1991) revolutionized the field by a series of seminal results, such as the Granger representation theorem stating that a cointegrated system set in discrete time has an autoregressive error correction model (ECM) representation. Similar results are available for continuous time systems, but modeling cointegration in continuous time is less popular in economics. Phillips (1991) introduced the concept of cointegartion in continuous time modeling and pointed out that the long-run parameters of a continuous time model can be estimated from discrete data by focusing on the corresponding discrete time ECM. Comte (1999) models cointegration in a continuous-time framework using CARMA (continuous-time autoregressive moving average) processes and develop a continuous time Granger representation theorem.

In this paper we develop a continuous time model of cointegrated commodity prices. This model features non-stationary commodity prices that are allowed be cointegrated. There is a vast literature on modelling the price of a single commodity as a non-stationary process. For example, Schwartz and Smith (2000) assume the log price to be the sum of two latent factors: the long-term equilibrium level, modeled as a geometric Brownian motion, and a short-term deviation from the equilibrium, modeled as a zero mean Ornstein - Uhlenbeck (OU) process. To account for higher order autoregressive and moving average components in the short-run deviation from equilibrium, Paschke and Prokopczuk (2010) propose to model these deviations as a more general CARMA process. Moreover, Cortazar and Naranjo (2006) generalizes the Schwartz and Smith (2000) model in a multi-factor framework. For an extensive account of the various types of one dimensional commodity price models, the reader is referred to the recent review of Back and Prokopczuk (2013). However, the literature on modeling a system of commodity prices is quite scarce.

Although cointegration has been studied well from a statistical and an econometric point of view, see e.g., Baillie and Myers (1991), Crowder and Hamed (1993) and Brenner and Kroner (1995), it has received little attention in the continuous-time asset pricing literature. Two fairly recent models, which are closly related to the one developed in this paper, are proposed

in Cortazar et al. (2008) and Paschke and Prokopczuk (2009), both of which account for cointegration by incorporating common and commodity-specific factors into their modeling framework. Amongst the common factors, only one is assumed non-stationary. Although they take into account explicitly that prices are cointegrated, the cointegrated sytems generated by these two models are not covering the whole range of possible number of contegration relations, but allow for none or for exactly $n-1$ relations to exist between the n prices.

Research on the pricing of derivatives written on cointegrated assets is understandably even scarcer. Duan and Pliska (2004) were (to the best of our knowledge) the first to examine the implications of cointegration for derivatives prices. They use a cointegrated multi-variate GARCH model to price options on the spread between two stocks. Their findings indicate that these prices only depend on the presence of cointegration when volatilities are stochastic. The recent paper by Nakajima and Ohashi (2012) also focuses on the implications of cointegration on spread options, but in contrast to Duan and Pliska (2004), they consider commodity rather than equity spread options. Their modeling approach is also somewhat different from Duan and Pliska (2004). Nakajima and Ohashi (2012) write the continuous-time model of Gibson and Schwartz (1990) down in a multi-variate cointegration framework. More specifically, they assume that the risk-neutral drift of a commodity spot log-price temporarily deviates from the risk-free rate, and that these deviations are described by convenience yields and cointegrating relations among the prices. Their primary finding is that – unlike the result of Duan and Pliska (2004) – cointegration affects the prices of commodity spread options no matter whether volatility is stochastic or not. This discrepancy in the findings of Duan and Pliska (2004) and Nakajima and Ohashi (2012) is due to the fact that stocks (unlike commodities) earn the risk-free rate under the pricing (or risk-neutral) measure.

Dempster et al. (2008) argue that when a cointegration relationship exists between two asset prices only the spread between the two should be modeled. This approach has the advantage that closed-form analytic pricing formulae for spread options may exist depending on the complexity of the dynamics. Dempster et al. (2008) obtain closed-form solutions under a two-factor Ornstein-Uhlenbeck (OU) process for the dynamics of the spot spread. However, this "direct" approach also presents certain drawbacks: since only the spread is modeled, it is not possible to obtain prices for futures and options on the individual components of the spread, nor is it possible to use market data on these derivatives. Furthermore, it is not straightforward to formulate the dynamics of the spread because it may, for example, reach negative values, but certainly not large negative values. An OU or square-root process would then not be appropriate choices.

To avoid these disadvantages, we follow Duan and Pliska (2004) and Nakajima and Ohashi (2012), among others, and model the dynamics of the (underlying) assets forming the spread. More specifically, we extend the modelling framework developed by Schwartz and Smith (2000). These two authors model the spot price dynamics of one commodity with two factors and show that their model is equivalent to the stochastic convenience-yield (SCY) model proposed by Gibson and Schwartz (1990). They do argue, however, that their specification better conforms with intuition than models based on the somewhat elusive notion of "convenience yield". Our extension of the Schwartz and Smith (2000) model to n commodities is parsimonious and intuitive. Just like Schwartz and Smith (2000), we use two factors to model the dynamics of the spot price of each commodity. Then, we assume that both factors are correlated across the n commodities, and that the long-term factor is also cointegrated across the n commodities. In contrast to the models mentioned above, our model can deal with one up to $n-1$ cointegration relationships, instead of only one (cf. Nakajima and Ohashi (2012)) or precisely $n-1$ (cf. Paschke and Prokopczuk (2009)). Furthermore, we argue that the idea of a cointegrated long-term (equilibrium) factor is more natural and intuitive than cointegrated convenience yields (cf. Duan and Pliska (2004), Cortazar et al. (2008)).

The model is estimated utilising data of futures prices for crude oil, heating oil, gasoline, natural gas and electric power. Compelling evidence is found of multiple cointegration relationships. For example, our results indicate that two cointegration relationships exist between crude oil, heating oil, gasoline and natural gas. Furthermore, we find evidence for cointegration between natural gas and electric power, and between electric power in various markets. To gain a better understanding of our model and of its implications for futures and spread options, we calculate the prices of futures and options written on the *spark spread*, the *crack spread* and on a spread between electric power prices in different markets, using the results of our model estimation. The results give a clear and concise overview of the implications of cointegration in commodity markets. Confirming previous work (cf., e.g., Nakajima and Ohashi (2012)), we find that cointegration alters the shape of term-structures of futures prices at long horizons. Furthermore, we find that cointegration creates an upward-sloping correlation term-structure. The latter finding is consistent with empirical evidence, but more importantly, it lowers the volatility of spreads, lowering therefore the prices of spread options.

The rest of the paper is organized as follows. In Section 1, we present the details of the model. Section 2 is devoted to deriving closed-form pricing formulae for futures and European-

style options. In Section 3, we estimate the model using data of futures prices for ten energy commodities. The purpose of Section 4 is to demonstrate the effects of cointegration on futures prices and spread option prices. Section 5 concludes.

1 Model for commodity spot prices

The model is constructed in such a way that it allows for several cointegration relations among the two factors driving the commodity prices in the system. The model also allows for obtaining closed-form prices of futures and European-style options. First, we start with a brief discussion of what the concept of cointegration entails.

Cointegration

Cointegration is a time-series property which was introduced by Engle and Granger (1987). Cointegration exists when a linear combination of two or more non-stationary time-series is stationary. To explain this by an example, let us suppose that $X_1(t)$ and $X_2(t)$ (where t denotes time) are two variables, then the time-series $\{X_1(t)\}_{t\in\mathcal{T}}$ and $\{X_2(t)\}_{t\in\mathcal{T}}$ (where $\mathcal{T}$ denotes a set of discrete time steps) are said to be cointegrated, when both are non-stationary, but a linear combination of them, say, $\{X_1(t) - \alpha X_2(t)\}_{t\in\mathcal{T}}$, is stationary for some $\alpha \in \mathbb{R}_{>0}$. In simply words, cointegration occurs when the paths of two or more variables (e.g. a pair or pool of stocks, interest rates or commodity futures) are linked to form a long-run equilibrium relationship from which they only temporarily depart.

Spot price model

Let $(\Omega, \mathcal{F}, \{\mathcal{F}_t\}_{t\geq 0}, \mathbb{P})$ be a filtered probability space satisfying the usual assumptions, where $\mathbb{P}$ denotes the statistical measure. We consider n commodity spot prices $\boldsymbol{S}(t) = (S_1(t), \ldots, S_n(t))^\top$ and denote $\boldsymbol{X}(t) = \log \boldsymbol{S}(t)$. Let $\widetilde{\boldsymbol{X}}(t) = \boldsymbol{X}(t) - \boldsymbol{\phi}(t)$ be the de-seasonalized log price process. Following Sorensen (2002), Paschke and Prokopczuk (2009), Nakajima and Ohashi (2012), the function $\boldsymbol{\phi}(t)$ is defined as follows:

$$\boldsymbol{\phi}(t) = \boldsymbol{\chi}_1 \cos(2\pi t) + \boldsymbol{\chi}_2 \sin(2\pi t), \tag{1}$$

where $\boldsymbol{\chi}_1$ and $\boldsymbol{\chi}_2$ are n-dimensional vectors of constants.[1] The process $\widetilde{\boldsymbol{X}}(t)$ is assumed to mean-revert towards a stochastic (non-stationary) long-run level $\boldsymbol{Y}(t)$, as specified by the following system of stochastic differential equations:

$$d\begin{bmatrix}\widetilde{\boldsymbol{X}}(t)\\ \boldsymbol{Y}(t)\end{bmatrix} = \begin{bmatrix}-K_x(\widetilde{\boldsymbol{X}}(t)-\boldsymbol{Y}(t))\\ \boldsymbol{\mu}_y - K_y\Theta\boldsymbol{Y}(t)\end{bmatrix}dt + \begin{bmatrix}\Sigma_x^{\frac{1}{2}} & \mathbf{O}_n\\ \Sigma_{xy}^{\frac{1}{2}} & \Sigma_y^{\frac{1}{2}}\end{bmatrix} d\begin{bmatrix}\boldsymbol{W}_x(t)\\ \boldsymbol{W}_y(t)\end{bmatrix} \tag{2}$$

where $\mathbf{O}_n$ refers to the matrix of size $n\times n$ full of zeros and $\boldsymbol{W} := (\boldsymbol{W}_x, \boldsymbol{W}_y)^\top$ is a $2n$-dimensional standard Brownian motion. Let us stress that there are n natural cointegration relationships assumed by equation (2): the n seasonally adjusted spot log-prices $\widetilde{\boldsymbol{X}}(t)$ are cointegrated with the corresponding elements of $\boldsymbol{Y}(t)$. The matrix K_x is an $n\times n$ matrix that quantifies the speed of mean reversion of the elements in $\boldsymbol{X}$ towards the long term levels in $\boldsymbol{Y}$. Note that the matrix K_x need not be diagonal. Intuitively we think of the two factors, $\boldsymbol{X}$ and $\boldsymbol{Y}$, as the short-end and the long-end of the term-structure of futures prices.

The main feature of our model is that it allows cointegration between the variables in $\boldsymbol{Y}(t)$. We denote the number of cointegration relationships between them by h, where $h\geq 0$ and $h<n$. The cointegration matrix Θ is an $n\times n$ matrix of rank h. Its last $n-h$ rows contain only zeros. Each of the h non-zero rows of Θ encodes a stationary (i.e., cointegrating) combination of the variables in $\boldsymbol{Y}(t)$, normalized such that $\Theta_{ii}=1,\ i\leq h$. The matrix K_y is a $n\times n$ matrix with the last $n-h$ columns filled with zeros, such that $K_y\Theta$ is a $n\times n$ matrix of rank h. Each of the h non-zero columns in K_y represents the speed of adjustment of each element in $\boldsymbol{Y}$ towards the corresponding cointegration relation.

Let us denote $\boldsymbol{Z}(t) = (\boldsymbol{X}(t)-\boldsymbol{\phi}(t), \boldsymbol{Y}(t))^\top$. The $n+h$ cointegration relationships between the variables in the $2n$-dimensional vector $\boldsymbol{Z}(t)$ can be characterized by the following $(2n\times 2n)$ cointegration matrix

$$\begin{bmatrix}\boldsymbol{I}_n & -\boldsymbol{I}_n\\ \mathbf{O}_n & \Theta\end{bmatrix} \tag{3}$$

[1] The seasonal behavior of energy commodity prices is documented, among others, by Manoliu and Tompaidis (2002), Borovkova and Geman (2006), Geman and Ohana (2009). As pointed out by Back et al. (2013), a deterministic seasonal component is not relevant for the pricing of commodity futures options, given observed futures prices. However, as noted by Lo and Wang (1995) and Back et al. (2013), a deterministic component in the price process might have a significant impact on the estimation of the model parameters, and, thereofore, indirectly on option prices.

and the dynamics of $\boldsymbol{Z}(t)$ can be written in short-hand notation as follows:

$$d\boldsymbol{Z}(t) = [\boldsymbol{\mu} - K\boldsymbol{Z}(t)]\,dt + \Sigma^{\frac{1}{2}} d\boldsymbol{W}(t), \tag{4}$$

which is a multi-variate Ornstein-Uhlenbeck (OU) process. Here the following definitions are used:

$$\boldsymbol{\mu} := \begin{bmatrix} \mathbf{0}_n \\ \boldsymbol{\mu}_y \end{bmatrix},\ K := \begin{bmatrix} K_x & -K_x \\ \mathbf{O}_n & K_y\Theta \end{bmatrix},\ \Sigma^{\frac{1}{2}} := \begin{bmatrix} \Sigma_x^{\frac{1}{2}} & \mathbf{O}_n \\ \Sigma_{xy}^{\frac{1}{2}} & \Sigma_y^{\frac{1}{2}} \end{bmatrix},\ \boldsymbol{W}(t) := \begin{bmatrix} \boldsymbol{W}_x(t) \\ \boldsymbol{W}_y(t) \end{bmatrix} \tag{5}$$

where $\mathbf{0}_n$ is a n-dimensional vector of zeros. If $h = n$, then the process $\boldsymbol{Z}(t)$ is stationary, and the model is said to be double-mean-reverting. If $h = 0$ then $\Theta = \mathbf{O}_n$ which corresponds to the two-factor model of Schwartz and Smith (2000).

The solution to (4) is given by:[2]

$$\boldsymbol{Z}(T) = \boldsymbol{Z}(t) + \left[e^{-K(T-t)} - \boldsymbol{I}_{2n}\right]\boldsymbol{Z}(t) + \left[\int_t^T e^{-K(T-u)}du\right]\boldsymbol{\mu} + \int_t^T e^{-K(T-u)}\Sigma^{\frac{1}{2}} d\boldsymbol{W}(u),$$

which means that $\boldsymbol{X}(T)$ can be written as:

$$\begin{aligned} \boldsymbol{X}(T) = \boldsymbol{X}(t) + [\boldsymbol{\phi}(T) - \boldsymbol{\phi}(t)] + \begin{bmatrix} \boldsymbol{I}_n & \mathbf{O}_n \end{bmatrix}\left[e^{-K(T-t)} - \boldsymbol{I}_{2n}\right]\boldsymbol{Z}(t) \\ + \begin{bmatrix} \boldsymbol{I}_n & \mathbf{O}_n \end{bmatrix}\left[\int_t^T e^{-K(T-u)}du\right]\boldsymbol{\mu} + \begin{bmatrix} \boldsymbol{I}_n & \mathbf{O}_n \end{bmatrix}\int_t^T e^{-K(T-u)}\Sigma^{\frac{1}{2}} d\boldsymbol{W}(u). \end{aligned} \tag{6}$$

Then using the result by Carbonell et al. (2008) that

$$e^{-K\tau} = \begin{bmatrix} e^{-K_x\tau} & \psi(\tau) \\ \mathbf{O}_n & e^{-K_y\Theta\tau} \end{bmatrix} \quad \text{with} \quad \psi(\tau) := K_x\left[\int_0^\tau e^{-K_x(\tau-u)}e^{-K_y\Theta u}du\right], \tag{7}$$

we obtain after straightforward calculations the following result:

$$\begin{aligned} \boldsymbol{S}(T) = \boldsymbol{S}(t)\exp\Bigg\{ &\left[e^{-K_x(T-t)} - \boldsymbol{I}_n\right]\boldsymbol{X}(t) + \psi(T-t)\boldsymbol{Y}(t) + \left[\phi(T) - e^{-K_x(T-t)}\phi(t)\right] \\ &+ \left[\int_t^T \psi(T-u)du\right]\mu_y + \int_t^T \left[e^{-K_x(T-u)}\Sigma_x^{\frac{1}{2}} + \psi(T-u)\Sigma_{xy}^{\frac{1}{2}}\right] d\boldsymbol{W}_x(u) \\ &+ \int_t^T \psi(T-u)\Sigma_y^{\frac{1}{2}} d\boldsymbol{W}_y(u)\Bigg\}. \end{aligned} \tag{8}$$

Our model belongs to the class of affine models proposed by Duffie and Kan (1996).

[2] Note that the matrix exponential of A is denoted by e^A and the element-by-element exponential of A by $\exp(A)$.

Therefore, the futures prices are exponentially affine in the two factors and the prices of European-style options are still given by a Black-like formula (see Black (1976)), which enables fast and efficient computations. The characteristic function of $\boldsymbol{X}(t)$ can be readily computed analytically, as shown in Lemma 1 in Appendix A.

Finally, we would like to stress that adding jumps by specifying a mean-reverting jump-diffusion process for $\boldsymbol{X}(t)$ (as in e.g. Hambly et al. (2009)) would not lead to other conclusions with respect to the effects of cointegration. The reason is that spot price jumps typically have a strong tendency to "mean-revert" (Hambly et al. (2009) find a jump mean-reversion rate that is many times higher than that of the purely diffusive part of $\boldsymbol{X}(t)$) and therefore only affect short-dated option prices, in contrast to cointegration which affects, essentially, only long-dated option prices.

2 Pricing of futures and European options

As there is no traded instrument that allows hedging the risks driving the components of the stochastic level of reversion vector $\boldsymbol{Y}$, the market is incomplete and the risk-neutral measure not unique. We parameterize the pricing kernel so that the market prices of risk be constant. The corresponding risk-neutral measure, equivalent to $\mathbb{P}$, is denoted by $\mathbb{Q}$. The dynamics of $\boldsymbol{Z}(t)$ under $\mathbb{Q}$ become:

$$d\boldsymbol{Z}(t) = [\boldsymbol{\mu}^* - K\boldsymbol{Z}(t)]\,dt + \Sigma^{\frac{1}{2}} d\boldsymbol{W}^*(t), \tag{9}$$

where $\boldsymbol{W}^*(t) := \begin{bmatrix} \boldsymbol{W}_x^*(t) \\ \boldsymbol{W}_y^*(t) \end{bmatrix}$, $\boldsymbol{W}_x^*(t)$ and $\boldsymbol{W}_y^*(t)$ are $\mathbb{Q}$ - Brownian motions, $\boldsymbol{\mu}^* = \begin{bmatrix} \boldsymbol{\mu}_x^* \\ \boldsymbol{\mu}_y^* \end{bmatrix} = \boldsymbol{\mu} - \Sigma^{\frac{1}{2}} \begin{bmatrix} \boldsymbol{\lambda}_x \\ \boldsymbol{\lambda}_y \end{bmatrix}$ and $\boldsymbol{\lambda}_x$, $\boldsymbol{\lambda}_y$ are the market prices of the two sources of risk.

We now readily obtain Proposition 1, which gives the "fair value" of a futures contract under the model.

Proposition 1. *At time t the price of a futures contract with maturity T is given by*

$$\boldsymbol{F}(t,T) = \exp\left\{\alpha(t,T) + \beta(T-t)\boldsymbol{X}(t) + \gamma(T-t)\boldsymbol{Y}(t)\right\}, \tag{10}$$

with $\beta(\tau) := e^{-K_x\tau}$, $\gamma(\tau) := \psi(\tau)$ *and with* $\alpha(t,T)$ *defined by*

$$\alpha(t,t+\tau) := \left[\phi(t+\tau) - e^{-K_x\tau}\phi(t)\right] + \left(\boldsymbol{I}_n - e^{-K_x\tau}\right) K_x^{-1}\boldsymbol{\mu}_x^* + \left(\int_0^\tau \psi(\tau-u)du\right)\boldsymbol{\mu}_y^* \quad (11)$$
$$+ \operatorname{diag}\left\{\frac{1}{2}\begin{bmatrix}\boldsymbol{I}_n & \boldsymbol{O}_n\end{bmatrix}\left[e^{-K\tau}\left(\int_0^\tau e^{Ku}\Sigma e^{Ku}du\right)e^{-K\tau}\right]\begin{bmatrix}\boldsymbol{I}_n \\ \boldsymbol{O}_n\end{bmatrix}\right\},$$

where $\operatorname{diag}(A)$ *returns the vector with diagonal elements of* A.

Proof. See Appendix B. **q.e.d.**

From Proposition (1), we see that the futures price $\boldsymbol{F}(t,T)$ is an exponential affine function of the two factors $\boldsymbol{X}(t)$ and $\boldsymbol{Y}(t)$. Note that, while the coefficients β and γ only depend on time t and maturity T through the (remaining) time to maturity $T-t$, α depends on both variables t and T independently (due to the seasonality function $\boldsymbol{\phi}(t)$).

By Itô's lemma the risk-neutral dynamics of $\boldsymbol{F}(t,T)$ are given by

$$\frac{d\boldsymbol{F}(t,T)}{\boldsymbol{F}(t,T)} = \left[e^{-K_x(T-t)}\Sigma_x^{\frac{1}{2}} + \psi(T-t)\Sigma_{xy}^{\frac{1}{2}}\right]d\boldsymbol{W}_x^*(t) + \psi(T-t)\Sigma_y^{\frac{1}{2}}d\boldsymbol{W}_y^*(t), \quad (12)$$

which immediately gives us the next proposition.

Proposition 2. *The variance-covariance matrix of returns on futures prices is given by:*

$$\Xi(\tau) = e^{-K_x\tau}\Sigma_x e^{-K_x^\top\tau} + \psi(\tau)\Sigma_{xy}^{\frac{1}{2}}(\Sigma_x^{\frac{1}{2}})^\top e^{-K_x^\top\tau} + e^{-K_x\tau}\Sigma_x^{\frac{1}{2}}(\Sigma_{xy}^{\frac{1}{2}})^\top\psi^\top(\tau) \quad (13)$$
$$+ \psi(\tau)\Sigma_{xy}\psi^\top(\tau) + \psi(\tau)\Sigma_y\psi^\top(\tau)$$

Proof. Follows immediately from (12). **q.e.d.**

Proposition 2 shows that unless $K_x = \mathbf{O}_n$, the variance-covariance matrix $\Xi(\tau)$ depends on τ.

Given that returns on futures prices follow a pure-diffusion process one can also readily obtain closed-form pricing formulae for plain vanilla options of European style. These formulae are given in Proposition 3 below.

Proposition 3. *The time-t price of a European-style call option with strike* k *and maturity* T *is given by*

$$c(t,F(t,T),k,T,v(t,T),r(t,T)) = e^{-r(t,T)(T-t)}\left[F(t,T)N(d_1) - KN(d_2)\right], \quad (14)$$

where $r(t,T)$ is the risk-free rate for maturity T. The parameters $d_{1,2}$ are given as usual by

$$d_{1,2} = \frac{\log(F(t,T)/K) \pm \frac{1}{2}v^2(t,T)(T-t)}{v(t,T)\sqrt{T-t}}, \tag{15}$$

where $v(t,T)$ in turn is given by

$$v(t,T) = \sqrt{\frac{1}{T-t}\int_t^T \Xi(T-s)ds}. \tag{16}$$

Proof. This is Black's formula (see Black (1976)). **q.e.d.**

3 Estimation results

The model is estimated on three sets of data. Data set I consists of weekly time-series data on the closing futures prices of 4 closely linked energy commodities, namely crude oil, heating oil, gasoline[3] and natural gas.[4] The contracts have maturities of 1, 3, 6, 9 and 12 months and are listed and traded on the NYMEX (New York Mercantile Exchange). The data span the period from January 1991 to December 2013.

Data set II is composed of weekly time-series data on the closing futures prices of electric power in 4 different markets, namely Germany, Nordics,[5] Switzerland and Poland.[6] These data cover a relatively short time period from January 2007 to December 2013.

Typically the most liquid and high-volume electric power futures contracts are the so-called Base Month, Base Quarter and Base Year ones. The Base Month is a contract delivering 720 MWh (megawatt-hours) for a period of 1 month (1MW $\times$ 30 days $\times$ 24 h/day = 720MWh). Base Quarter (Year) contracts are nothing else than a series of 3 (12) consecutive Base Month contracts.

To make the model compatible with the data in set II we regard 720 MWh electric power for a period of 1 month as a commodity, and we shall henceforth refer to it as the **power commodity**. Note that we have 4 power commodities, one for each region. The power commodity serves as the underlying asset for the Base Month contract. The theoretical (or model) futures prices of the Base Month contract can be easily calculated by using (10). The

[3] From January 1991 to December 2005 data on Unleaded Gasoline (HU) is used, while data on Reformulated Blendstock for Oxygenate Blending (RB) is used for the remainder of the period (i.e., for the period January 1996 to December 2013). The reason is that the HU contracts stopped trading on NYMEX end of 2005. We note that the HU and RB contracts were trading at almost the same prices over the 2-year period they co-existed.

[4] This data set was retrieved from Quandl (www.quandl.com).

[5] The Nordics consist of Sweden, Norway, Denmark, Finland, Iceland, The Faroe Island and Greenland.

[6] This data set was obtained from the trading division of AXPO AG.

Base Quarter contract is, as noted earlier, a bundle of 3 Base Month contracts with maturities T, $T+1M$ and $T+2M$ (capital "M" means month). Similarly, the Base Year contract with maturity T is a bundle of 12 Base Month contracts with maturities T, $T+1M$, ..., $T+10M$ and $T+11M$. It follows therefore that the price of a Base Quarter (Base Year) contract is simply given by the average of the prices of 3 (12) Base Month contracts. For each type of contract (i.e., Base Month, Base Quarter and Base Year), we only use the data on the nearest futures contracts. The reason is that on some days and for some regions only one maturity is available.

Data set III comprises weekly time-series data on the closing prices of electric power (Phelix Base Futures) and natural gas (TTF Natural Gas Futures) futures contracts, both of which are traded on the EEX (European Energy Exchange).[6] The data cover the time period from January 2006 to December 2013. The reason for not taking the weekly natural gas futures prices from data set I and/or the weekly electric power futures prices from data set II is simply because these data cannot be (straightforwardly) used to compute values of the *spark spread* (which is defined as the spread between the market price of electric power and the cost of the natural gas needed to produce that electric power). The "power commodity" in data set III corresponds to electric power for one day and the "natural gas commodity" corresponds precisely to the amount of natural gas needed to generate that much electricity, which enables an easy calculation of the spark spread.

Since the state variables $\boldsymbol{X}(t)$ and $\boldsymbol{Y}(t)$ cannot be observed directly from the data, they must be inferred from the (observable) futures prices. We use the Kalman filter for this purpose.[7] The state (or transition) equation is given by (2). The measurement equation is obtained by adding a n-dimensional (uncorrelated) Gaussian noise term to the right-hand side of (10). We stress that the Kalman filter is applicable because the transition and measurement equation are subject to Gaussian noise and linear in $\boldsymbol{X}(t)$ and $\boldsymbol{Y}(t)$. The Kalman filter is also used for computing the likelihood of the (observed) futures prices given the model and the model parameters. This facilitates a straightforward maximum likelihood (ML) estimation of the model parameters.

Given that there are a large number of parameters, we employ a two-step ML estimation procedure. In the first step, we estimate a simple one-dimensional version of the model for each commodity separately. The estimates for the parameters of the seasonality term (1), as well as those for the variance of the measurement errors, are kept fixed in the second step. The estimates for the other parameters serve as starting point for the second step of

[7] We refer the reader to Kalman (1960) or Welch and Bishop (1995) for more details about the Kalman filter.

the estimation procedure. The filtered values of the latent state variables $\boldsymbol{X}(t)$ and $\boldsymbol{Y}(t)$ are utilized to calculate reasonable starting values for parameters that cannot be estimated within the model version used in step one (i.e., correlation and cointegration parameters).

In the second step of the estimation procedure, the parameters of the full model are estimated (with exception of those that are kept fixed at values obtained in the first step). This time the log-likelihood function is maximized under the restriction that the model is "well-specified". Specifically, this means that at each iteration (of our maximization routine) we perform a Johansen constraint test,[8] checking whether the cointegration properties of the filtered time-series of $\boldsymbol{X}(t)$ and $\boldsymbol{Y}(t)$ do not contradict with the cointegration matrix Θ.

From now onwards we present and discuss the estimation results. Figures 17 through 26 (Appendix C) show the time-series of the spot log-prices $\boldsymbol{X}(t)$ and the long-run log-price levels $\boldsymbol{Y}(t)$, both of which were filtered from the data. For all 10 commodities, we observe that the spot log-prices $\boldsymbol{X}(t)$ fluctuate quite wildly around the long-run log-price levels $\boldsymbol{Y}(t)$, which themselves are also varying over time (but with a lower magnitude, as expected). The bottom panels (of Figures 17 through 26) depict the seasonality patterns we found in the data. We note from these results that there is a very noticeable seasonality in the (futures) prices of heating oil, gasoline and the 4 power commodities with the exception of "power Poland". The seasonality seen in crude oil prices seems negligible.

For comparison reasons, the 10 long-run log-price levels $\boldsymbol{Y}(t)$ are also shown in Figures 1 through 3. Figure 1 suggests that the long-run log-price levels of crude oil, heating oil and gasoline are driven by only one factor. This would mean that no less than 2 cointegration relationships exist among these 3 variables. The long-run log-price level of natural gas, however, seems to be driven by another factor. These visual findings are confirmed by the estimated cointegration matrix (see (17)), denoted by $\hat{\Theta}_I$ for data set I, by $\hat{\Theta}_{II}$ for data set II, and by $\hat{\Theta}_{III}$ for data set III.[9]

[8] The Johansen test (see Johansen (1991)) is a procedure for testing the presence of cointegration relationships between two or more time-series.

[9] Statistical significance at 1% symbolized by ***, statistical significance at 5% symbolized by ** and statistical significance at 10% symbolized by *

$$\hat{\Theta}_I = \begin{bmatrix} 1.00 & -0.69^{***} & -0.28^{***} & 0.03^{***} \\ 0.36^{***} & 1.00 & -1.47^{***} & 0.05 \\ 0.00 & 0.00 & 0.00 & 0.00 \\ 0.00 & 0.00 & 0.00 & 0.00 \end{bmatrix}, \quad \hat{\Theta}_{II} = \begin{bmatrix} 1.00 & -1.33^{***} & 0.00 & 0.00 \\ 0.00 & 1.00 & -0.63^{***} & 0.00 \\ 0.00 & 0.00 & 1.00 & -0.74^{***} \\ 0.00 & 0.00 & 0.00 & 0.00 \end{bmatrix}, \tag{17}$$

$$\hat{\Theta}_{III} = \begin{bmatrix} 1.00 & -2.27^{***} \\ 0.00 & 0.00 \end{bmatrix}.$$

It is clear from Figure 2 that the long-run log-price levels of power in the 4 regions are driven by only one factor. Intuitively this also makes sense because one would expect that price differences between regions (or countries) stabilize in the long-run. This visual finding is also confirmed by the estimated cointegration matrix $\hat{\Theta}_{II}$.

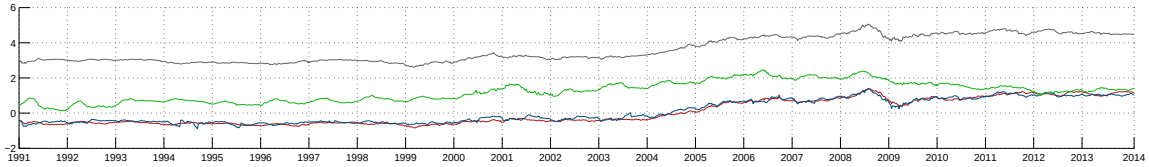

Figure 1. Filtered time-series of the long-run log-price levels $\boldsymbol{Y}(t)$ (data set I). The colors corresponds to the following 4 commodities: gray (crude oil), red (heating oil), blue (gasoline), and green (natural gas).

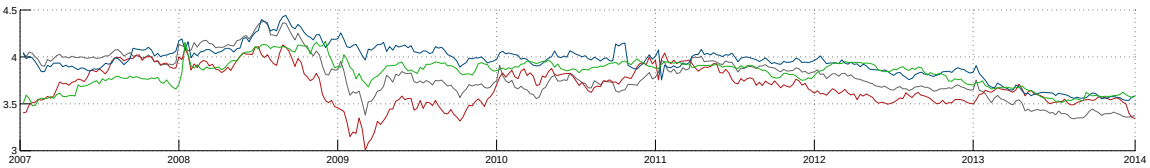

Figure 2. Filtered time-series of the long-run log-price levels $\boldsymbol{Y}(t)$ (data set II). The colors corresponds to the following 4 commodities: gray (power Germany), red (power Nordics), blue (power Swiss), and green (power Poland).

Figure 3. Filtered time-series of the long-run log-price levels $\boldsymbol{Y}(t)$ (data set III). The colors corresponds to the following 2 commodities: gray (electric power) and red (natural gas).

For the sake of completeness, we also report the estimates of the parameters other than

Θ. Values of these estimates can be found in Appendix C. Most of these results are well-known, and are hence not covered in detail here. We only mention a few results that we find interesting.

Recall that the matrices K_x and K_y measure the speed at which $\boldsymbol{X}(t)$ and $\boldsymbol{Y}(t)$ return to their co-integrated equilibria. From the estimates of K_x and K_y, we see that $\boldsymbol{X}(t)$ returns at least twice as fast to its equilibrium state than $\boldsymbol{Y}(t)$. This is a very intuitive result, because a deviation of $\boldsymbol{X}(t)$ from its "equilibrium" value is likely due to daily fluctuations in supply and demand (or speculative activity) whereas a deviation of $\boldsymbol{Y}(t)$ from its "equilibrium" value is more likely due to structural shifts in supply and demand.

A second observation is that $\boldsymbol{X}(t)$ and $\boldsymbol{Y}(t)$ are strongly positively correlated, as indicated by the estimates of Σ_{xy}. This result is again very intuitive if we recall that $\boldsymbol{X}(t)$ and $\boldsymbol{Y}(t)$ correspond to the short-end and the long-end of the term-structure of futures prices, which typically have a strong tendency to co-move (as evidenced by many empirical studies).

Finally, the fact that the elements of $\boldsymbol{\lambda}_y$ are, in general, positive proves that the risks associated with changes in the $\boldsymbol{Y}(t)$'s are priced. The values of the $\boldsymbol{\lambda}_x$'s give a mixed result. This means that investing in long-term futures contracts provides an extra return (in excess of the risk-free rate) to compensate for the risks involved, but the same might not be true for short-term futures contracts.

4 Prices for spread options

In this section we derive prices of European-style options written on the price difference, or *spread*, between two or more commodities. Spread options present an ideal setting for investigating the implications of cointegration, since they crucially depend on the short- and long-run relation between the assets that make up the spread. Also, since spread options have become regularly and widely-used instruments in financial markets for e.g. hedging purposes or for exploiting (statistical) arbitrage opportunities, there is a growing need for a better understanding of the effects of cointegration on their prices.

We will distinguish between options on spreads between 2 commodities and options on spreads between $n > 2$ commodities. The reason is that for the 2-commodity case we have analytic (approximation) formulas, such as Margrabe's formula (see Margrabe (1978)) and Kirk's (approximation) formula (see Kirk (1995)), while for the general case (i.e., when $n > 2$) we have to rely on numerical methods.[10]

[10] Also for the $n = 3$ case there are some (semi-)analytic approximation formulas, such as the extension of Kirk's formula proposed by Alos et al. (2011), but here we give preference to the Monte-Carlo technique.

The 2-commodity case

The holder of a European-style call option on the spread between 2 commodities receives at maturity T the pay-off

$$\max(S_1(T) - \alpha S_2(T) - k, 0), \tag{18}$$

where k is the strike price, and where $\alpha > 0$ is usually the ratio of the units of measure of $S_1(t)$ to the units of measure of $S_2(t)$ or, in case of an "input-output" (or production) spread (e.g., crack, dark or spark spread), the input-output conversion rate. When the strike price k equals zero a spread option is equivalent to an option to exchange one asset for another. In this special case, the price of the option can be computed analytically by Margrabe's formula (see Margrabe (1978)). In the general case, however, there are no closed-form pricing formulae for spread options (at least to the best of our knowledge). Instead, we need to rely on approximation formulae or extensive numerical computations.

For the 2-commodity case considered here we utilize the formula derived by Kirk (1995). Kirk's formula approximates the time-t price of a spread option with pay-off (18) by

$$c(t, F_1(t,T), \alpha F_2(t,T) + k, T, \widetilde{v}(t,T), r(t,T)), \tag{19}$$

where $c(\cdot)$ is Black's formula given in Proposition 3, and where the volatility $\widetilde{v}(t,T)$ is given by

$$\widetilde{v} = \sqrt{v_1^2 - 2\frac{\alpha F_2}{\alpha F_2 + k}\rho v_1 \alpha v_2 + \left[\frac{\alpha F_2}{\alpha F_2 + k}\right]^2 \alpha^2 v_2^2}. \tag{20}$$

The dependence on t and T has been suppressed here for clarity.

Note that Kirk's formula coincides with Margrabe's formula when the strike price k equals zero. Alternative approximation formulae can be found in Carmona and Durrleman (2003) and Bjerksund and Stensland (2011). These formulae typically improve upon Kirk's formula in terms of numerical accuracy and efficiency, but they come at the cost of higher computational complexity. Since for our purpose the precision of Kirk's formula is sufficient we keep the formulae simple here and not use any of these alternative ones.

First, we present a simple example to have a better grasp on the influence of various parameters on futures prices and the variance of spreads.

Example 1 (*spreads between two commodities*)**.** Consider two commodities having a single

cointegration relation between their long term components given by $Y_1 - \theta Y_2$ with $\theta > 0$ and $\mathbb{E}[Y_1 - \theta Y_2] = 0$. Therefore, the cointegration matrix is $\Theta = \begin{bmatrix} 1 & -\theta \\ 0 & 0 \end{bmatrix}$. We also assume a simple specification for the dynamics given by $\boldsymbol{\chi}_1 = \boldsymbol{\chi}_2 = \mathbf{0}_2$, $\boldsymbol{\mu}_y = \mathbf{0}_2$, $\boldsymbol{\lambda}_x = \boldsymbol{\lambda}_y = \mathbf{0}_2$, $K_x = \begin{bmatrix} k_1 & 0 \\ 0 & k_2 \end{bmatrix}$, with $k_1, k_2 > 0, K_y = \begin{bmatrix} l_1 & 0 \\ -l_2 & 0 \end{bmatrix}$, with $l_1, l_2 > 0$, $\Sigma_x = \begin{bmatrix} \sigma_x^2 & 0 \\ 0 & \sigma_x^2 \end{bmatrix}$, $\Sigma_y = \begin{bmatrix} \sigma_y^2 & 0 \\ 0 & \sigma_y^2 \end{bmatrix}$, and $\Sigma_{xy} = \mathbf{O}_2$. At a time t, the long run distribution of $\boldsymbol{X}$, that is the distribution of $\boldsymbol{X}(t+\tau)$ when τ is large, is given by

$$\boldsymbol{X}(t+\tau) \sim \mathcal{N}\left(\Psi_1 \boldsymbol{Y}(t) + o(\tau), \sigma_y^2 \Psi_2 \tau + o(\tau)\right) \tag{21}$$

with $\Psi_1 := \begin{bmatrix} \frac{l_2\,\theta}{l_1 + l_2\,\theta} & \frac{l_1\,\theta}{l_1 + l_2\,\theta} \\ \frac{l_2}{l_1 + l_2\,\theta} & \frac{l_1}{l_1 + l_2\,\theta} \end{bmatrix}, \Psi_2 := \begin{bmatrix} \frac{\theta^2\left({l_1}^2 + {l_2}^2\right)}{(l_1 + l_2\,\theta)^2} & \frac{\theta\left({l_1}^2 + {l_2}^2\right)}{(l_1 + l_2\,\theta)^2} \\ \frac{\theta\left({l_1}^2 + {l_2}^2\right)}{(l_1 + l_2\,\theta)^2} & \frac{{l_1}^2 + {l_2}^2}{(l_1 + l_2\,\theta)^2} \end{bmatrix}$. Although the covariance matrices of the shocks are diagonal, the presence of the cointegration between the two commodities induces a positive correlation between them in the long run. Analogously, the long run distribution of $\boldsymbol{Y}$ is

$$\boldsymbol{Y}(t+\tau) \sim \mathcal{N}\left(\Psi_1 \boldsymbol{Y}(t) + o(\tau), \sigma_y^2 \Psi_2 \tau + o(\tau)\right). \tag{22}$$

One can easily notice that $X_1 - \theta X_2$ is stationary since its mean and variance no longer depend on τ. On the other hand, $X_1 - \alpha X_2$ with $\alpha \neq \theta$ is not stationary and one has that

$$VAR(X_1(t+\tau) - \alpha X_2(t+\tau)) = \sigma_y^2 (\theta - \alpha)^2 \frac{1 + l^2}{(l + \theta)^2} \tau + o(\tau) \tag{23}$$

where $l := \frac{l_1}{l_2}$. The variance of the spread is at its minimum when $l = \frac{1}{\theta}$.

However, when it comes to spread options one is interested in spreads between prices and not between log prices. The mean and variance of a spread $S_1 - \alpha S_2$ can be easily computed using the properties of the multivariate log-normal distribution. Next, we fix $\alpha = 1$, $\theta = 1.25$, $k_1 = k_2 = 2$, $\sigma_x^2 = 0.2$, $\sigma_y^2 = 0.05$, $\boldsymbol{X}(0) = \begin{bmatrix} 3.69 \\ 2.95 \end{bmatrix}$, $\boldsymbol{Y}(0) = \begin{bmatrix} 3.60 \\ 2.90 \end{bmatrix}$ and run a simulation to assess the impact of parameters l_1 and l_2 on the 10 years futures spread, on the correlation of the futures log-returns between the two components of the spread at 10 years maturity, on the volatility $\widetilde{v}$ for a 10 years horizon and on the at-the-money (ATM) European-style call spread option prices with 10 years to maturity. The spot price of the spread at time 0 is 20.94. For the sake of clarity we have set the risk-free rate curve $r(t, \cdot)$

equal to zero.

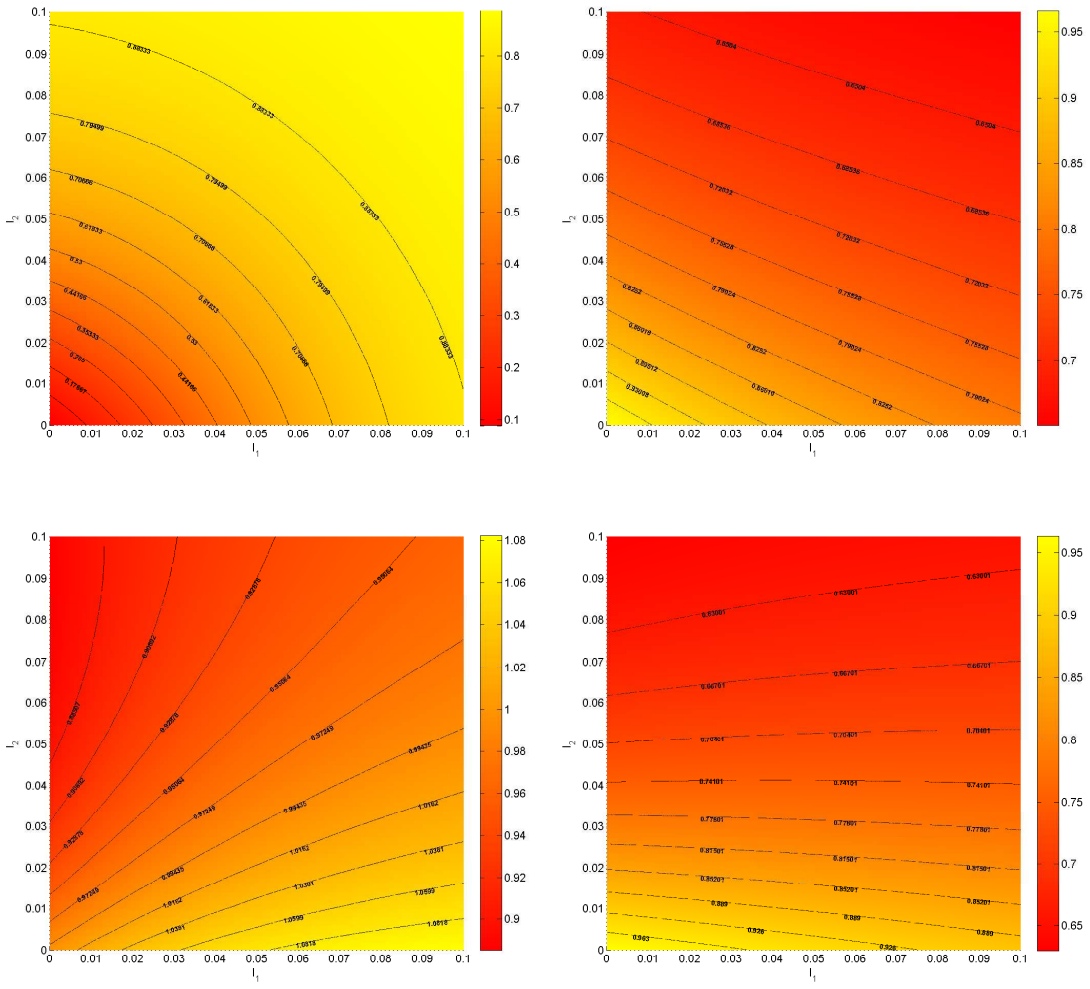

Figure 4. Top left panel: Correlation between the 10 years futures log-returns. **Top right panel:** Kirk volatility at 10 years. **Bottom left panel:** 10 years spread futures prices. **Bottom right panel:** 10 years ATM option prices. *Note:* The volatilities, the futures prices and the option prices are normalized with respect to the case of no cointegration.

Figure 4 display the impact on the four quantities when one varies l_1, l_2 from 0 to 0.1. When there is cointegration and the dynamics of the variables responds to the deviations in the cointegration relation the correlation between the two components of the spread increases and the volatility of the spread decreases, both implying lower option prices. Indeed, the ATM option price when $l_1 = l_2 = 0.1$ is almost 35% lower than in the case when the cointegration relation is not accounted for (i.e. $l_1 = l_2 = 0$). It is quite easy to run Monte Carlo simulations of futures prices in our model (as explained in the next subsection). Using such a simulation, Figure 5 compares the distribution at maturity (10 years) of the spread between the case

there is no cointegration between the long term components of the commodities ($l_1 = l_2 = 0$) and the case when $l_1 = l_2 = 0.1$.

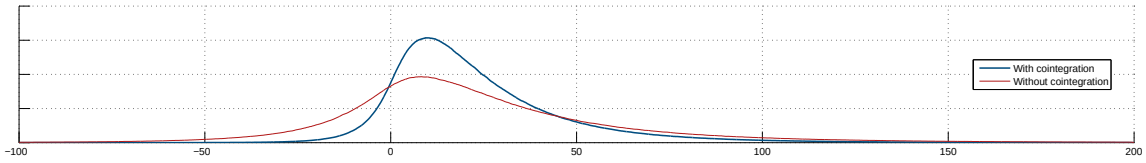

Figure 5. The distribution of the spread at maturity

The variance of the spread is higher when there is no cointegration mainly because the correlation between the two components of the spread is zero in this case since we assumed the covariance matrices of the shocks are diagonal.

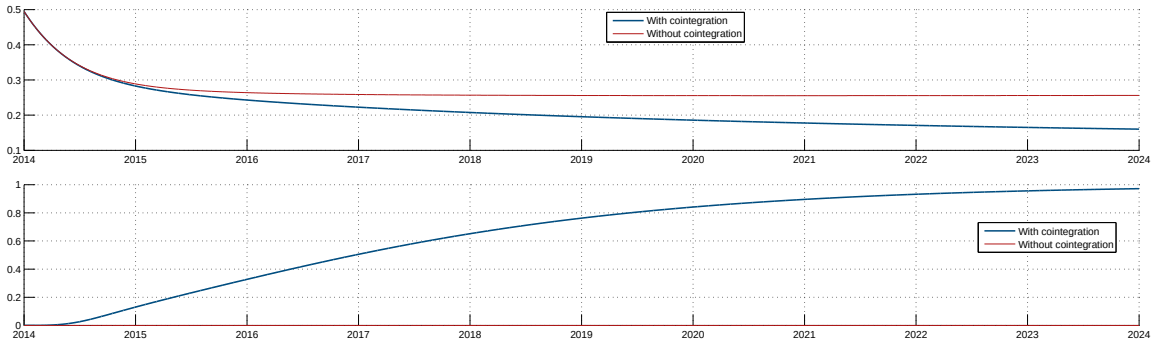

Figure 6. Top panel: Kirk's volatility $\widetilde{v}(t,T)$ as a function of maturity time T. **Bottom panel:** Correlation between the futures log-returns of both commodities. *Note:* The blue line corresponds to the original model, the red line to the model with no cointegration between the n variables in $\boldsymbol{Y}(t)$.

To see this we look at Figure 6, where Kirk's volatility $\widetilde{v}(t,T)$ (see (20)) is plotted as a function of maturity time T. No differences between the two cases (with and without cointegration in $\boldsymbol{Y}(t)$) up to $T = 2015$, but for $T > 2015$ we clearly see a substantially larger volatility for the case without cointegration in $\boldsymbol{Y}(t)$. This reduction in volatility is caused mainly by a stronger correlation between the futures log-returns of both commodities when there is cointegration in $\boldsymbol{Y}(t)$ (see the bottom panel of Figure 6), which is intuitive, since in this case the far long-end of the term-structure is driven by only one factor. The term structure of futures prices and of ATM call option prices are shown in Figures 7 and 8. Figure 8 is the same as Figure 7, except that here no cointegration between the n variables in $\boldsymbol{Y}(t)$ is assumed.

From Figure 7, we observe again a significant impact of seasonality on the results. This is the reason why we also plotted the results for the case without seasonality (depicted by gray lines). Let us now consider the shapes of the term-structures of futures prices. For

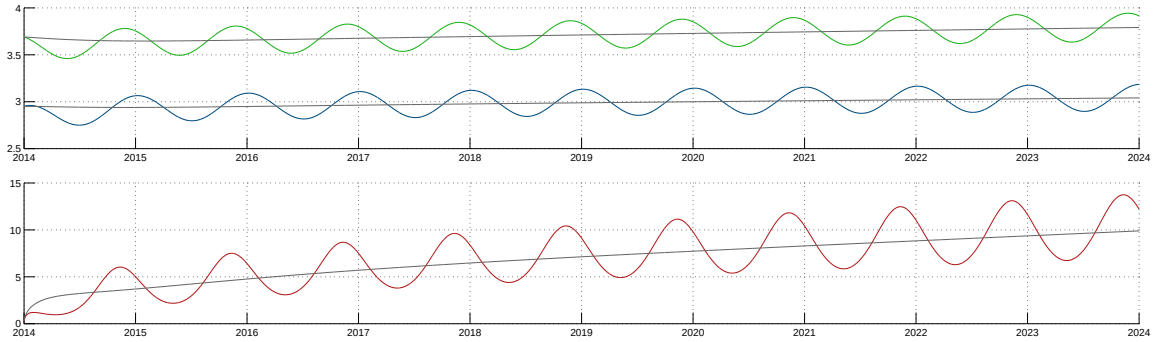

Figure 7. Top panel: Term-structure of futures log-prices for power (green line) and gas (blue line). **Bottom panel:** Term-structure of spark spread option prices. *Note:* The gray lines indicate the case without seasonality effects.

Figure 8. Top panel: Term-structure of futures log-prices for power (green line) and gas (blue line). **Bottom panel:** Term-structure of spark spread option prices. *Note:* The gray lines indicate the case without seasonality effects.

that, it is important to note that these term-structures depict exactly how spot prices would evolve in absence of stochasticity (something that is also clear from the definition of futures prices, see (30)). As a consequence, the term-structures are subject to the same influences as the spot prices $\boldsymbol{S}(t)$, namely (i) the reversion of the seasonally adjusted spot log-prices $\boldsymbol{X}(t) - \boldsymbol{\phi}(t)$ towards their long-run levels $\boldsymbol{Y}(t)$ and (ii) the reversion of the latter towards their co-integrated "equilibrium" relationship(s) (characterized by the matrix Θ). Since the speed of reversion "(i)" is greater than that of reversion "(ii)" (see also the discussion in Section 3 above), "(i)" primarily influences the short-end of the term structures while "(ii)" primarily influences the long-end of the term structures. This is also clearly reflected in the figures: Up to a maturity of one year the shape of the term-structures is clearly determined by "(i)", that is, the one-year seasonally adjusted futures log-prices are relatively close to $\boldsymbol{X}(t = 2014) = (3.69, 2.95)^\top$. For maturities longer than one-year we see a convergence towards the cointegration "equilibrium" levels, i.e., $K_y \Theta \log \boldsymbol{F}(t = 2014, T = 2024) \approx \boldsymbol{\mu}_y$. This also explains why the term-structures in Figure 7 are very similar (to the ones in Figure

8) up to $T = 2015$ but differ for larger T. Spread option prices are plotted in the bottom panel of Figures 7 and 8. An immediate observation is that those in Figure 7 (with cointegration in $\boldsymbol{Y}(t)$) are substantially lower than those in Figure 8 (without cointegration in $\boldsymbol{Y}(t)$) and this is, as discussed above, mainly due to a lower variance of the spread because of positive correlation induced by cointegration.

We will now present another example on spreads between two commodities in which a so-called *spark spread* option is priced. In this example, we rely on the estimation results for data set III (see Section 3).

Example 2 (*spark spread*)**.** The spark spread is, as mentioned, the spread between the market price of electric power and the cost of the natural gas needed to produce that electric power. As such, the spark spread is a metric of the profitably of natural gas-fired electric power plants. Hence, utility companies employ the spark spread as an indicator for turning on or off their natural gas-fired electric power plants. When this is not possible (in the short-term), they often resort to buying (financial) futures and/or options on the spark spread to hedge their risk of a profit margin squeeze. In this example, the prices of these two types of instruments are calculated using the estimation results of data set III.

The spot price of the spark spread at January 1st 2014 (according to our model) is \$8.87. Using Kirk's formula, we now compute the price of an at-the-money (ATM), hence $k = 8.87$, European-style call option with maturities up to 10 years starting January 1st 2014. For the sake of clarity we have set the vector of risk premiums $\boldsymbol{\lambda}_x$ and $\boldsymbol{\lambda}_y$ and the risk-free rate curve $r(t, \cdot)$ equal to zero. The results are shown in Figures 9 and 10. Figure 10 is the same as Figure 9, except that here no cointegration between the n variables in $\boldsymbol{Y}(t)$ is assumed.

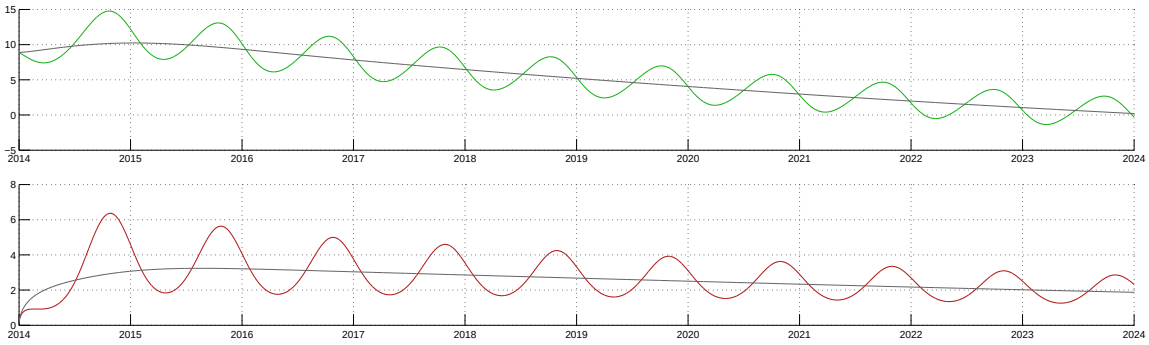

Figure 9. Top panel: Term-structure of spread futures. **Bottom panel:** Term-structure of spark spread option prices. *Note:* The gray lines indicate the case without seasonality effects.

The shapes of the term-structures of spread futures prices and that of the ATM option prices are similar in the two cases since the estimated speeds of reverting to the cointegration

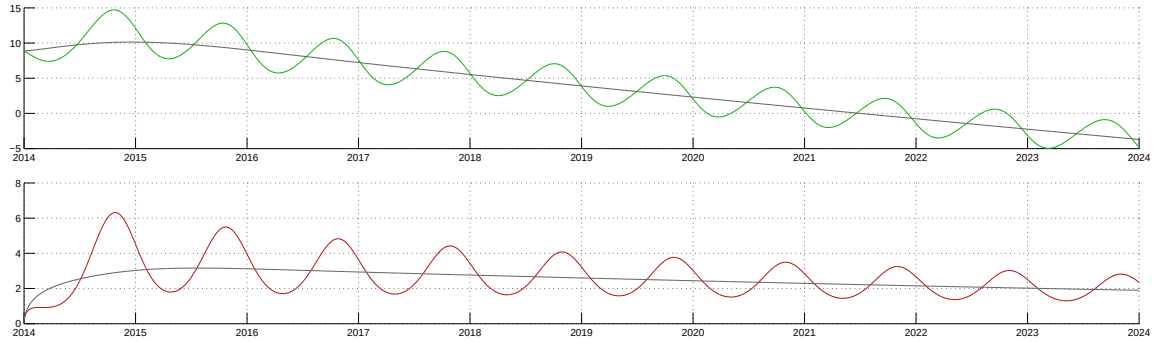

Figure 10. Top panel: Term-structure of spread futures. **Bottom panel:** Term-structure of spark spread option prices. *Note:* The gray lines indicate the case without seasonality effects.

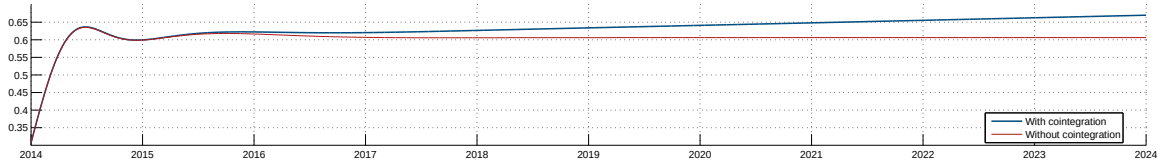

Figure 11. Correlation between the futures log-returns of both commodities. *Note:* The blue line corresponds to the original model, the red line to the model with no cointegration between the n variables in $\boldsymbol{Y}(t)$.

relation (i.e. the elements of K_y) are both close to zero and not statistically significant. The effect of cointegration is most visible in the term-structure of the correlation of the futures log-returns between the two components of the spark spread, depicted in Figure 11. In contrast to the previous example, the correlation of the futures log-returns is strictly positive even in the absence of cointegration. This is due to the fact that the estimated covariance matrix of the shocks is not diagonal. However, cointegration induces additional correlation that is increasing with maturity.

The n-commodity case

There is an extensive literature on approximation methods for spread and basket options on more that two commodities, with recent contributions from Li et al. (2010) and Caldana and Fusai (2013). However, mostly for simplicity, we relay in this paper on the Monte-Carlo simulation method for pricing spread options written on more than two commodities. We briefly describe how the Monte-Carlo method is applied to our problem. For more general details we refer the reader to Binder (1987).

From (12), it follows that $\boldsymbol{F}(t,T)$ (conditional on information available up to time $s \leq$

$t \leq T$) is distributed as follows:

$$\boldsymbol{F}(t,T) \sim \log\mathcal{N}\left(\log \boldsymbol{F}(s,T) - \frac{1}{2}\int_s^t \Xi(T-u)du, \int_s^t \Xi(T-u)du\right), \tag{24}$$

where $\boldsymbol{F}(s,T)$ can be readily computed theoretically from (10) but may emerge from the data as well.

The fact that the distribution function of $\boldsymbol{F}(t,T)$ is known in an easy-to-use and analytic form is one of the merits of our model. It allows us to simulate futures price curves at any time t in the future based on today's curves (time s) almost effortlessly. Hence, the price of a call option on the time-T value of a certain spread can be simply obtained by carrying out the following steps:

(i) compute or observe today's futures price curves $\boldsymbol{F}(s,T)$;

(ii) compute M realisations $\boldsymbol{F}^{(m)}$ $(m = 1,\ldots,M)$ of $\boldsymbol{F}(T,T)$ by sampling from (24) as follows:

$$\boldsymbol{F}^{(m)} = \boldsymbol{F}(s,T)\exp\left\{-\frac{1}{2}\int_s^T \Xi(T-u)du + \left[\int_s^T \Xi(T-u)du\right]^{\frac{1}{2}}\boldsymbol{\varepsilon}^{(m)}\right\},$$

where $\boldsymbol{\varepsilon}^{(m)}$ is a vector of randomly generated independent standard normal random variables;[11]

(iii) compute the Monte-Carlo estimate of a call with strike k on the spread

$$S_1(T) - \sum_{n=2}^N \omega_n S_n(T) \qquad \left(= F_1(T,T) - \sum_{n=2}^N \omega_n F_n(T,T)\right),$$

with $\omega_n \in \mathbb{R}_{\geq 0}$ for all $n = 2,\ldots,N$, as follows:

$$\frac{1}{M}\sum_{m=1}^M \max\left\{F_1^{(m)} - \left[\sum_{n=2}^N \omega_n F_n^{(m)}\right] - k, 0\right\}. \tag{25}$$

We note that the random variables $\boldsymbol{\varepsilon}^{(m)}$ can be simply re-used for pricing spread options with different maturity dates.

Example 3 considers the pricing of an option on the *crack spread*, which is a spread between the futures prices of 3 commodities. This example will rely on the estimation results

[11] Here the technique of antithetic variables is used to reduce the number of random samples needed for a given level of accuracy.

for data set I (see Section 3).

Example 3 (*crack spread option*)**.** The crack spread refers in general to the price difference between crude oil and refined products such as diesel, kerosine, gasoline and petroleum. The crack spread is hence nothing else than the profit margin that an oil refiner realizes when "cracking" crude oil while simultaneously selling the refined products in the wholesale market.

In this example we will consider a so-called 3:2:1 crack spread, which consists of shorting 3 crude oil futures contracts and purchasing 2 gasoline futures contracts and 1 heating oil futures contract. Since gasoline and heating oil are quoted in dollars-per-gallon while crude oil, and usually also the crack spread, is quoted in dollars-per-barrel, we must multiply the futures prices of gasoline and heating oil by 42 (the number of gallons per barrel). The crack spread is therefore calculated as follows:

$$-3 \times F_{\text{crude oil}}(t,T) + 2 \times 42 \times F_{\text{gasoline}}(t,T) + 42 \times F_{\text{heating oil}}(t,T). \tag{26}$$

An oil refiner can hedge the risk of losing profits by buying an appropriate number of futures contract on the crack spread. However, then he also loses any upside. As an alternative the oil refiner can buy a call option of the crack spread. Then he pays a fixed up-front cost (premium), but still profits from any future widening of the spread. In the following, we will calculate the prices of futures and call options on the crack spread using the estimation results of data set I.

The spot price of the spread at January 1st 2014 (according to our model) is \$65.52. Now we price an (out-of-the-money) European-style call option with strike $K = \$250.00$ on the crack spread with maturities up to 10 years starting January 1st 2014. For this purpose we rely on the Monte-Carlo based method presented above. The results are summarized in Figures 12 through 14. Like Figure 10, Figure 13 shows the case where there is no cointegration between the variables in $\boldsymbol{Y}(t)$.

The spread option prices are significantly lower when cointegration is accounted for. To better understand the latter observation, we have plotted in Figure 14 the probability distribution of the spread 10 years out. We find that the shape of the distribution is wider without cointegration and gets narrower when the cointegration relations are included in the model. The variance of the crack spread distribution is lower in the model with cointegration given higher positive correlations between the three components. Indeed, Figure 15 depict the effect of cointegration on the term-structure of the correlation of the futures log-returns between the three components of the crack spread. Again, the correlation of the futures log-

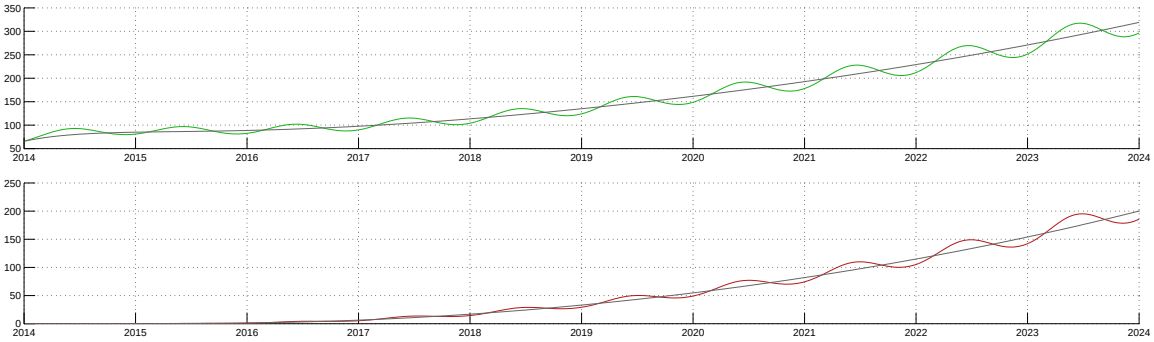

Figure 12. Top panel: Term-structure of futures crack spread prices. **Bottom panel:** Term-structure of crack spread option prices. *Note:* The gray lines indicate the case without seasonality effects.

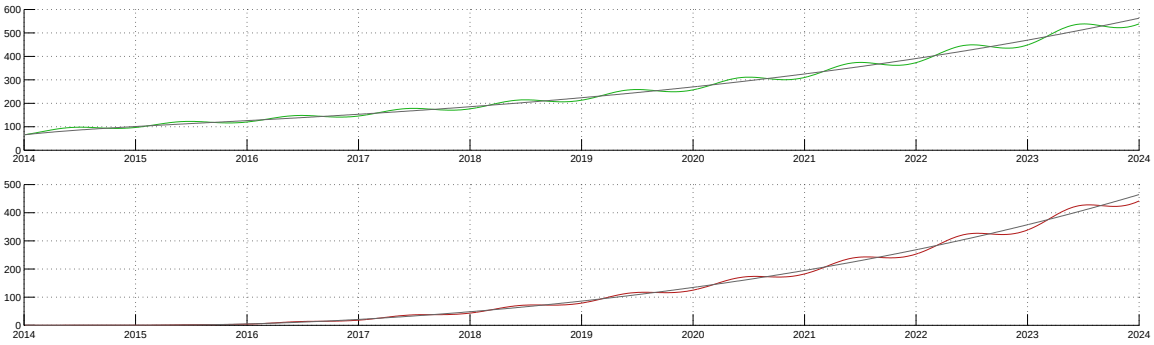

Figure 13. Top panel: Term-structure of futures crack spread prices. **Bottom panel:** Term-structure of crack spread option prices. *Note:* The gray lines indicate the case without seasonality effects.

returns is strictly positive even in the absence of cointegration. However, the correlations in the model without cointegration quickly reduces during approximatively the first three years. On the other hand, the additional correlation induced by cointegration is increasing with maturity.

Finally, we present an example of a spread between four commodities. In this example, we rely on the estimation results for data set II (see Section 3).

Example 4 (*power spread*)**.** Consider a spread between the price of electric power on the Swiss market and the average between the prices of electric power in the German, Nordic and Polish markets:

$$F_{\text{Switzerland}}(t,T) - 0.33 \times \left(F_{\text{Germany}}(t,T) + F_{\text{Nordics}}(t,T) + F_{\text{Poland}}(t,T)\right). \tag{27}$$

The spot price of the spread at January 1st 2014 according to our model is 13.19.

Figure 16 depicts the distribution of the spread 10 years in the future. Again, the shape of

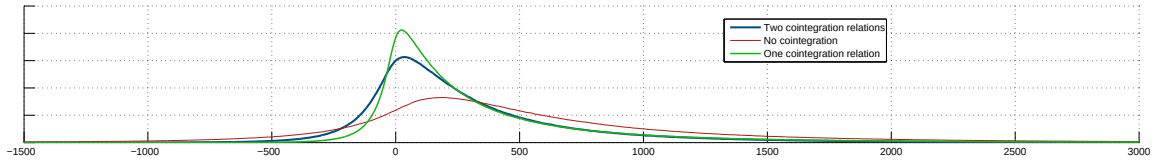

Figure 14. The distribution of the crack spread 10-years out.

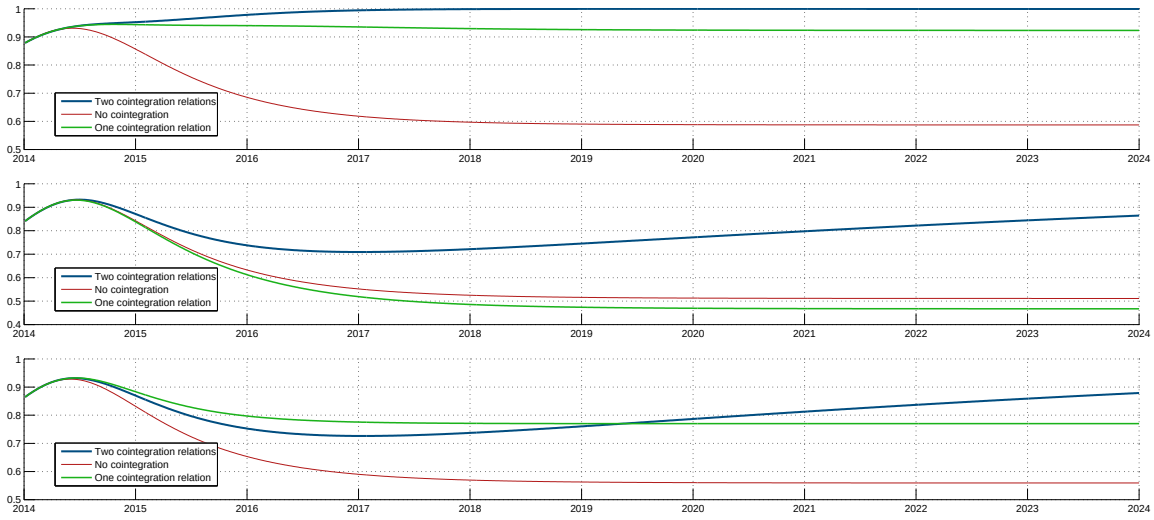

Figure 15. Correlation between the futures log-returns of three commodities (from top to bottom: between 1 and 2, between 2 and 3, between 1 and 3). *Note:* The blue line corresponds to the original model, the red line to the model with no cointegration between the n variables in $\boldsymbol{Y}(t)$, and the green line to the model with only the first cointegration relation between the n variables in $\boldsymbol{Y}(t)$.

the distribution is wider if cointegration is not taken into consideration. This has of course a significant impact on option prices. For example, the price of a ATM call on the spread with 10 years to maturity is three times higher in the model without cointegration. As in the previous examples, the lower variance of the spread distribution in the model with cointegration is due to higher positive correlations between the four components.

5 Conclusion

We have presented a two-factor model for commodity spot prices. As in Schwartz and Smith (2000), one factor captures short-term price fluctuations while another captures the long-term ones. In contrast to Schwartz and Smith (2000), however, our model is applicable to an n-commodity economy. Following a fairly recent trend in the literature (cf. Duan and Pliska (2004), Paschke and Prokopczuk (2009), Cortazar et al. (2008) and Nakajima and Ohashi (2012)), we allow for co-integrated variables in our model. More specifically, we assume that the spot price is fully cointegrated with the long-term factor and that the long-term factors are

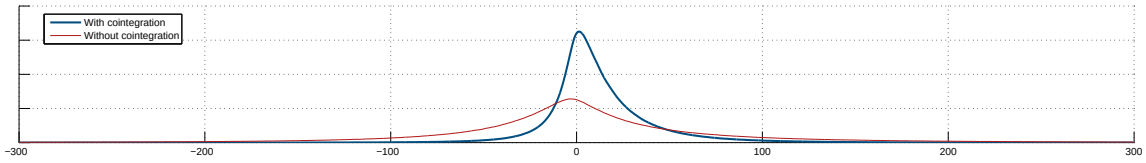

Figure 16. The distribution of the power spread 10-years in the future.

cointegrated across commodities. As opposed to Paschke and Prokopczuk (2009) and Cortazar et al. (2008), our model is capable of describing one up to $n-1$ cointegration relationships between the long-term factors of n commodities. The models of Duan and Pliska (2004) and Nakajima and Ohashi (2012) could also be extended to include more than one cointegration relationship but both models are defined in a convenience yield framework, which hinders a transparent analysis (as also pointed out by Schwartz and Smith (2000)).

We have estimated our model using three alternative data sets. First, we used weekly futures prices of crude oil, heating oil, gasoline and natural gas with a wide range of maturities, spanning a period of over twenty years. We found two (statistically significant) cointegration relationships. Only natural gas is not co-integrated with one of the others. Second, we again used weekly futures prices, but now of electric power in four different regions. As expected, we found that all of them are strongly cointegrated with each other. The third data set consisted of futures prices on electric power and natural gas, and also here we found a cointegration relationship.

Using the estimation results of our model, we have calculated the prices of several spread options on energy commodities. The purpose here was merely to illustrate the effects of cointegration. We found that cointegration affects the entire but particularly the long-end of futures price term-structures. Furthermore, we found that cointegration leads to an upward sloping correlation term-structure which lowers the volatility of spreads and therefore it also lowers the value of options on spreads.

References

Alos, E., Eydeland, A., and Laurence, P. (2011). A Kirk and a Bachelier formula for three asset spread options. *Energy Risk*, 9(2011):52–57.

Back, J. and Prokopczuk, M. (2013). Commodity price dynamics and derivative valuation: A review. *International Journal of Theoretical and Applied Finance*, 16(6):1350032.

Back, J., Prokopczuk, M., and Rudolf, M. (2013). Seasonality and the valuation of commodity options. *Journal of Banking & Finance*, 37:273ñ290.

Baillie, R. T. and Myers, R. J. (1991). Bivariate garch estimation of the optimal commodity futures hedge. *Journal of Applied Econometrics*, 6(2):109–124.

Binder, K. (1987). Monte carlo methods. *Quantum Monte Carlo Methods*, page 241.

Bjerksund, P. and Stensland, G. (2011). Closed form spread option valuation. *Quantitative Finance*, (ahead-of-print):1–10.

Black, F. (1976). Studies of stock price volatility changes. In *Proceedings of the 1976 Meetings of the American Statistical Association*, pages 171–181.

Borovkova, S. and Geman, H. (2006). Seasonal and stochastic effects in commodity forward curves. *Review of Derivatives Research*, 9:167 – 186.

Brenner, R. J. and Kroner, K. F. (1995). Arbitrage, cointegration, and testing the unbiasedness hypothesis in financial markets. *Journal of Financial and Quantitative Analysis*, 30(01):23–42.

Caldana, R. and Fusai, G. (2013). A general closed-form spread option pricing formula. *Journal of Banking & Finance*, 37:4893ñ4906.

Carbonell, F., Jimenez, J., and Pedroso, L. (2008). Computing multiple integrals involving matrix exponentials. *Journal of Computational and Applied Mathematics*, 213(1):300–305.

Carmona, R. and Durrleman, V. (2003). Pricing and hedging spread options. *Siam Review*, 45(4):627–685.

Comte, F. (1999). Discrete and continuous time cointegration. *Journal of Econometrics*, 88(2):207–226.

Cortazar, G., Milla, C., and Severino, F. (2008). A multicommodity model of futures prices: Using futures prices of one commodity to estimate the stochastic process of another. *Journal of Futures Markets*, 28(6):537–560.

Cortazar, G. and Naranjo, L. (2006). An N-factor gaussian model of oil futures prices. *Journal of Futures Markets*, 26(3):243ñ268.

Crowder, W. J. and Hamed, A. (1993). A cointegration test for oil futures market efficiency. *Journal of Futures Markets*, 13(8):933–941.

Dempster, M., Medova, E., and Tang, K. (2008). Long term spread option valuation and hedging. *Journal of Banking & Finance*, 32(12):2530–2540.

Duan, J.-C. and Pliska, S. R. (2004). Option valuation with co-integrated asset prices. *Journal of Economic Dynamics and Control*, 28(4):727–754.

Duffie, D. and Kan, R. (1996). A yield-factor model of interest rates. *Mathematical Finance*, 6:379–406.

Engle, R. F. and Granger, C. W. (1987). Co-integration and error correction: representation, estimation, and testing. *Econometrica*, pages 251–276.

Geman, H. and Ohana, S. (2009). Forward curves, scarcity and price volatility in oil and natural gas markets. *Energy Economics*, 31:576 – 585.

Gibson, R. and Schwartz, E. S. (1990). Stochastic convenience yield and the pricing of oil contingent claims. *The Journal of Finance*, 45(3):959–976.

Hambly, B., Howison, S., and Kluge, T. (2009). Modelling spikes and pricing swing options in electricity markets. *Quantitative Finance*, 9(8):937–949.

Johansen, S. (1991). Estimation and hypothesis testing of cointegration vectors in gaussian vector autoregressive models. *Econometrica*, pages 1551–1580.

Kalman, R. E. (1960). A new approach to linear filtering and prediction problems. *Journal of Fluids Engineering*, 82(1):35–45.

Kirk, E. (1995). Correlation in the energy markets. *Managing energy price risk*, pages 71–78.

Li, M., Zhou, J., and Deng, S.-J. (2010). Multi-asset spread option pricing and hedging. *Quantitative Finance*, 10(3):305ñ324.

Lo, A. and Wang, J. (1995). Implementing option pricing models when asset returns are predictable. *Journal of Finance*, 50:87ñ129.

Manoliu, M. and Tompaidis, S. (2002). Energy futures prices: term structure models with Kalman filter estimation. *Applied Mathematical Finance*, 9:21 – 43.

Margrabe, W. (1978). The value of an option to exchange one asset for another. *The Journal of Finance*, 33(1):177–186.

Nakajima, K. and Ohashi, K. (2012). A cointegrated commodity pricing model. *Journal of Futures Markets*, 32(11):995–1033.

Paschke, R. and Prokopczuk, M. (2009). Integrating multiple commodities in a model of stochastic price dynamics. *Journal of Energy Markets*, 2(3):47ñ82.

Paschke, R. and Prokopczuk, M. (2010). Commodity derivatives valuation with autoregressive and moving average components in the price dynamics. *Journal of Banking & Finance*, 34:2742 – 2752.

Phillips, P. (1991). Error correction and long-run equilibrium in continuous time. *Econometrica*, 59(4):967–980.

Schwartz, E. and Smith, J. E. (2000). Short-term variations and long-term dynamics in commodity prices. *Management Science*, 46(7):893–911.

Sorensen, C. (2002). Modeling seasonality in agricultural commodity futures. *Journal of Futures Markets*, 22(5):393ñ426.

Welch, G. and Bishop, G. (1995). An introduction to the kalman filter.

A Lemmas

Lemma 1. *The characteristic function of* $\boldsymbol{X}(t+\tau)$ *conditional on the information up to and including time* t*, i.e.,*

$$\varphi_{\boldsymbol{X}}(t,\tau,x,y;\omega) := \mathbb{E}_t\left[\exp\left\{i\omega^\top \boldsymbol{X}(t+\tau)\right\}|\boldsymbol{X}(t)=x,\boldsymbol{Y}(t)=y\right], \tag{28}$$

is given by[12]

$$\begin{aligned}\varphi_{\boldsymbol{X}}(t,\tau,x,y;\omega) = \exp\Big\{ & i\omega^\top e^{-K_x\tau}x + i\omega^\top\psi(\tau)y + i\omega^\top\left[\phi(t+\tau)-e^{-K_x\tau}\phi(t)\right] \\ & + i\omega'\left[\int_0^\tau \psi(\tau-u)du\right]\boldsymbol{\mu}_y \\ & - \frac{1}{2}\left(\omega^\top,\mathbf{0}\right)^\top\left[e^{-K\tau}\left(\int_0^\tau e^{Ku}\Sigma e^{K^\top u}du\right)e^{-K^\top\tau}\right]\left(\omega',\mathbf{0}\right)^\top\Big\}.\end{aligned} \tag{29}$$

Proof. By straightforward calculations. **q.e.d.**

B Proof of Proposition 1

By the no-arbitrage assumption, the j-th futures price is given by

$$F_j(t,T) = \mathbb{E}_t^*\left[S_j(T)\right] = \mathbb{E}_t^*\left[\exp(X_j(T))|\boldsymbol{X}(t)=\boldsymbol{x},\boldsymbol{Y}(t)=\boldsymbol{y}\right] = \varphi_{\boldsymbol{X}}^*(t,\tau,x,y;-i\omega_j). \tag{30}$$

where $\varphi_{\boldsymbol{X}}^*(\cdot)$ is the characteristic function of $\boldsymbol{X}(T)$ under the risk-neutral measure, and where ω_j is a n-dimensional vector with the j-th component equal to 1 and the other components equal to 0. Noting that $\varphi_{\boldsymbol{X}}^*(\cdot)$ is similar to $\varphi_{\boldsymbol{X}}(\cdot)$ (see Lemma 1) but with $\boldsymbol{\mu}$ replaced by $\boldsymbol{\mu}^*$, we find

$$\begin{aligned}F_j(t,T) = \exp\Big\{ & \omega_j^\top e^{-K_x\tau}\boldsymbol{X}(t) + \omega_j^\top\psi(\tau)\boldsymbol{Y}(t) + \omega_j^\top\left[\phi(t+\tau)-e^{-K_x\tau}\phi(t)\right] \\ & + \omega_j^\top\left[\int_0^\tau e^{-K_x(\tau-u)}du\right]\mu_x^* + \omega_j^\top\left[\int_0^\tau\psi(\tau-u)du\right]\mu_y^* \\ & + \frac{1}{2}\begin{bmatrix}\omega_j^\top & \mathbf{0}_n^\top\end{bmatrix}\left[e^{-K\tau}\left(\int_0^\tau e^{Ku}\Sigma e^{Ku}\right)e^{-K^\top\tau}\right]\begin{bmatrix}\omega_j^\top \\ \mathbf{0}_n\end{bmatrix}\Big\}.\end{aligned}$$

The proposition can be verified now by a straightforward calculation.

[12] The integrals appearing here can be computed explicitly using results in Carbonell et al. (2008).

C Estimation results

Below we report the parameter estimates [13] for data set I, II and III where $\widetilde{\boldsymbol{\lambda}} := \Sigma^{\frac{1}{2}}\boldsymbol{\lambda}$ and $\Sigma := \begin{bmatrix} diag(\sigma_x) & \mathbf{O}_n \\ \mathbf{O}_n & diag(\sigma_y) \end{bmatrix} \begin{bmatrix} \rho_x & \rho_{xy} \\ \rho_{xy}{}^{\top} & \rho_y \end{bmatrix} \begin{bmatrix} diag(\sigma_x) & \mathbf{O}_n \\ \mathbf{O}_n & diag(\sigma_y) \end{bmatrix}$.

Data set I:

$$\hat{\mu}_x = \begin{bmatrix} 0.00 \\ 0.00 \\ 0.00 \\ 0.00 \end{bmatrix}, \; \hat{\widetilde{\boldsymbol{\lambda}}}_x = \begin{bmatrix} 0.10^{***} \\ 0.08^{***} \\ 0.13^{***} \\ -0.10^{***} \end{bmatrix}, \; \hat{K}_x = \begin{bmatrix} 1.18^{***} & 0.01 & 0.02^{**} & 0.01 \\ 0.04 & 1.18^{***} & 0.01 & -0.01 \\ 0.00 & 0.03 & 1.05^{***} & 0.00 \\ 0.00 & 0.00 & 0.00 & 2.48^{***} \end{bmatrix},$$

$$\hat{\sigma}_x = \begin{bmatrix} 0.35^{***} \\ 0.34^{***} \\ 0.34^{***} \\ 0.60^{***} \end{bmatrix}, \; \hat{\rho}_x = \begin{bmatrix} 1.00 & 0.88^{***} & 0.86^{***} & 0.26^{***} \\ 0.88^{***} & 1.00 & 0.84^{***} & 0.34^{***} \\ 0.86^{***} & 0.84^{***} & 1.00 & 0.26^{***} \\ 0.26^{***} & 0.34^{***} & 0.26^{***} & 1.00 \end{bmatrix}, \; \hat{\mu}_y = \begin{bmatrix} 2.27^{***} \\ -1.88^{***} \\ -0.29 \\ -2.68^{**} \end{bmatrix}, \; \hat{\widetilde{\boldsymbol{\lambda}}}_y = \begin{bmatrix} 0.13^{***} \\ 0.12^{***} \\ 0.15^{***} \\ 0.05 \end{bmatrix},$$

$$\hat{K}_y = \begin{bmatrix} 0.64^{***} & -0.11^{***} & 0.00 & 0.00 \\ -0.60^{***} & 0.12 & 0.00 & 0.00 \\ -0.10 & -0.03 & 0.00 & 0.00 \\ -0.76^{**} & 0.01 & 0.00 & 0.00 \end{bmatrix}, \; \hat{\Theta} = \begin{bmatrix} 1.00 & -0.69^{***} & -0.28^{***} & 0.03^{***} \\ 0.36^{***} & 1.00 & -1.47^{***} & 0.05 \\ 0.00 & 0.00 & 0.00 & 0.00 \\ 0.00 & 0.00 & 0.00 & 0.00 \end{bmatrix},$$

$$\hat{\sigma}_y = \begin{bmatrix} 0.23^{***} \\ 0.19^{***} \\ 0.28^{***} \\ 0.24^{***} \end{bmatrix}, \; \hat{\rho}_y = \begin{bmatrix} 1.00 & 0.59^{***} & 0.56^{***} & 0.08 \\ 0.59^{***} & 1.00 & 0.51^{***} & 0.28^{***} \\ 0.56^{***} & 0.51^{***} & 1.00 & 0.16^{**} \\ 0.08 & 0.28^{***} & 0.16^{**} & 1.00 \end{bmatrix}, \; \hat{\rho}_{xy} = \begin{bmatrix} 0.48^{***} & 0.64^{***} & 0.50^{***} & 0.22^{***} \\ 0.58^{***} & 0.52^{***} & 0.53^{***} & 0.22^{***} \\ 0.53^{***} & 0.62^{***} & 0.29^{***} & 0.22^{***} \\ 0.20^{***} & 0.10^{**} & 0.14^{***} & 0.37^{***} \end{bmatrix},$$

$$\hat{\boldsymbol{\chi}}_1 = \begin{bmatrix} 0.00 \\ 0.03^{***} \\ -0.04^{***} \\ -0.01^{***} \end{bmatrix}, \; \hat{\boldsymbol{\chi}}_2 = \begin{bmatrix} 0.00 \\ -0.01^{***} \\ 0.02^{***} \\ 0.01^{***} \end{bmatrix}.$$

[13] Statistical significance at 1% symbolized by ***, statistical significance at 5% symbolized by ** and statistical significance at 10% symbolized by *.

Data set II:

$$\hat{\mu}_x = \begin{bmatrix} 0.00 \\ 0.00 \\ 0.00 \\ 0.00 \end{bmatrix},\ \hat{\tilde{\boldsymbol{\lambda}}}_x = \begin{bmatrix} -0.58^{***} \\ -0.05 \\ -0.08 \\ 0.07 \end{bmatrix},\ \hat{K}_x = \begin{bmatrix} 1.59^{***} & 0.39 & 0.20^{***} & -0.02 \\ -1.37^{**} & 2.55^{***} & -0.24 & 0.35^{*} \\ -4.51^{***} & 1.27^{***} & 4.95^{***} & -0.26 \\ -0.40 & 0.17 & -0.13 & 1.38^{***} \end{bmatrix},$$

$$\hat{\sigma}_x = \begin{bmatrix} 0.33^{***} \\ 0.51^{***} \\ 0.43^{***} \\ 0.23^{***} \end{bmatrix},\ \hat{\rho}_x = \begin{bmatrix} 1.00 & 0.25^{***} & 0.61^{***} & 0.24^{***} \\ 0.25^{***} & 1.00 & 0.25^{***} & 0.27^{***} \\ 0.61^{***} & 0.25^{***} & 1.00 & 0.27^{***} \\ 0.24^{***} & 0.27^{***} & 0.27^{***} & 1.00 \end{bmatrix},\ \hat{\mu}_y = \begin{bmatrix} 0.92^{***} \\ 0.87^{***} \\ 0.21 \\ 0.01 \end{bmatrix},\ \hat{\tilde{\boldsymbol{\lambda}}}_y = \begin{bmatrix} 0.27^{*} \\ 0.30 \\ 0.22^{*} \\ 0.11 \end{bmatrix},$$

$$\hat{K}_y = \begin{bmatrix} 0.78^{***} & 1.20^{***} & 0.25^{***} & 0.00 \\ -0.81^{***} & 0.00 & -0.05 & 0.00 \\ 0.24^{**} & 0.00 & 0.37^{***} & 0.00 \\ -0.17 & -0.19^{***} & 0.00 & 0.00 \end{bmatrix},\ \hat{\Theta} = \begin{bmatrix} 1.00 & -1.33^{***} & 0.00 & 0.00 \\ 0.00 & 1.00 & -0.63^{***} & 0.00 \\ 0.00 & 0.00 & 1.00 & -0.74^{***} \\ 0.00 & 0.00 & 0.00 & 0.00 \end{bmatrix},$$

$$\hat{\sigma}_y = \begin{bmatrix} 0.34^{***} \\ 0.42^{***} \\ 0.32^{***} \\ 0.29^{***} \end{bmatrix},\ \hat{\rho}_y = \begin{bmatrix} 1.00 & 0.72^{***} & 0.60^{***} & 0.38^{***} \\ 0.72^{***} & 1.00 & 0.42^{***} & 0.48^{***} \\ 0.60^{***} & 0.42^{***} & 1.00 & 0.24^{***} \\ 0.38^{***} & 0.48^{***} & 0.24^{***} & 1.00 \end{bmatrix},\ \hat{\rho}_{xy} = \begin{bmatrix} -0.01 & -0.10 & 0.02 & -0.14 \\ 0.39^{***} & 0.37^{***} & 0.45^{***} & 0.17^{**} \\ 0.32^{***} & 0.21 & 0.14^{***} & 0.08 \\ 0.25^{**} & 0.15^{*} & 0.22^{*} & 0.28^{***} \end{bmatrix},$$

$$\hat{\boldsymbol{\chi}}_1 = \begin{bmatrix} 0.14^{***} \\ 0.13^{***} \\ 0.20^{***} \\ -0.01^{***} \end{bmatrix},\ \hat{\boldsymbol{\chi}}_2 = \begin{bmatrix} -0.01 \\ 0.01 \\ 0.01 \\ 0.02^{***} \end{bmatrix}.$$

Data set III:

$$\hat{\mu}_x = \begin{bmatrix} 0.00 \\ 0.00 \end{bmatrix},\ \hat{\tilde{\boldsymbol{\lambda}}}_x = \begin{bmatrix} -0.59^{***} \\ -0.36^{**} \end{bmatrix},\ \hat{K}_x = \begin{bmatrix} 0.94^{**} & 0.60^{**} \\ -4.15^{***} & 2.41^{***} \end{bmatrix},\ \hat{\sigma}_x = \begin{bmatrix} 0.30^{***} \\ 0.46^{***} \end{bmatrix},\ \hat{\rho}_x = \begin{bmatrix} 1.00 & 0.31^{***} \\ 0.31^{***} & 1.00 \end{bmatrix},$$

$$\hat{\mu}_y = \begin{bmatrix} -0.06 \\ 0.02 \end{bmatrix},\ \hat{\tilde{\boldsymbol{\lambda}}}_y = \begin{bmatrix} 0.17^{*} \\ 0.52^{***} \end{bmatrix},\ \hat{K}_y = \begin{bmatrix} 0.00 & 0.00 \\ -0.02 & 0.00 \end{bmatrix},\ \hat{\Theta} = \begin{bmatrix} 1.00 & -2.27^{***} \\ 0.00 & 0.00 \end{bmatrix},\ \hat{\sigma}_y = \begin{bmatrix} 0.18^{***} \\ 0.30^{***} \end{bmatrix},$$

$$\hat{\rho}_y = \begin{bmatrix} 1.00 & 0.61^{***} \\ 0.61^{***} & 1.00 \end{bmatrix},\ \hat{\rho}_{xy} = \begin{bmatrix} 0.25^{**} & -0.33^{***} \\ 0.44^{***} & 0.20 \end{bmatrix},\ \hat{\boldsymbol{\chi}}_1 = \begin{bmatrix} 0.12^{***} \\ 0.14^{***} \end{bmatrix},\ \hat{\boldsymbol{\chi}}_2 = \begin{bmatrix} -0.09^{***} \\ 0.01 \end{bmatrix}.$$

Figures 17 through 24 show values of the filtered $\boldsymbol{X}(t)$ and $\boldsymbol{Y}(t)$ and those of the estimated seasonal component.

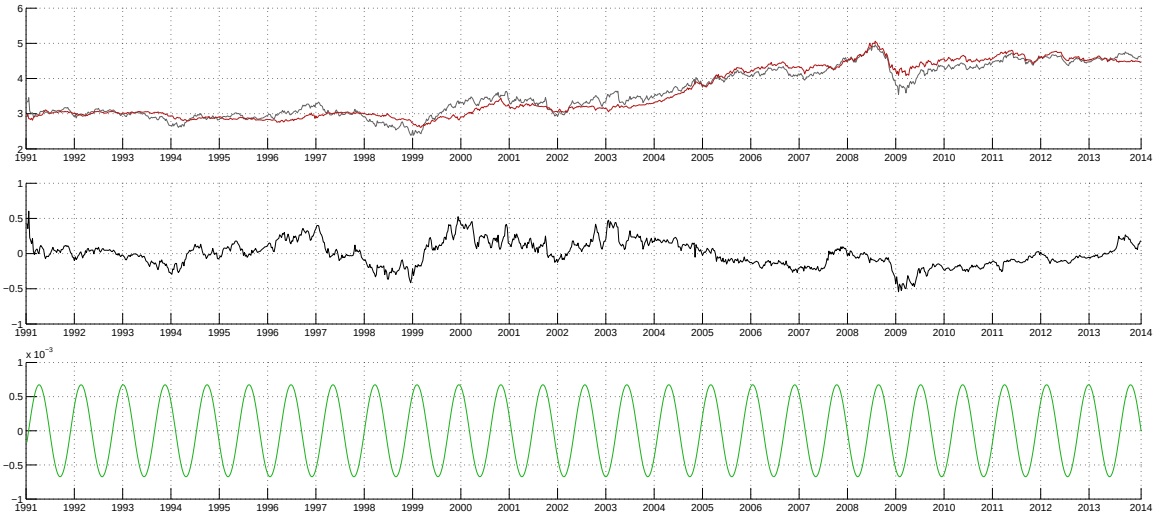

Figure 17. Top panel: Filtered time-series of spot log-prices $\boldsymbol{X}(t)$ (gray line) and long-run log-price level $\boldsymbol{Y}(t)$ (red line) for **crude oil**. **Middle panel:** Differences between short- and long-term log-price levels, i.e., $\boldsymbol{X}(t) - \phi(t) - \boldsymbol{Y}(t)$. **Bottom panel:** Estimated seasonality function for **crude oil**.

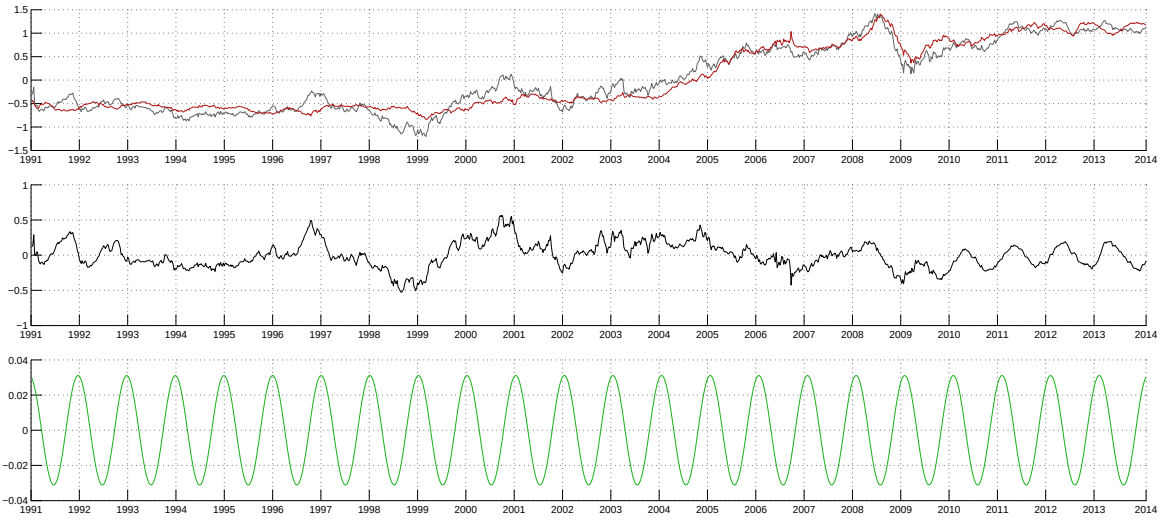

Figure 18. Top panel: Filtered time-series of spot log-prices $\boldsymbol{X}(t)$ (gray line) and long-run log-price level $\boldsymbol{Y}(t)$ (red line) for **heating oil**. **Middle panel:** Differences between short- and long-term log-price levels, i.e., $\boldsymbol{X}(t) - \phi(t) - \boldsymbol{Y}(t)$. **Bottom panel:** Estimated seasonality function for **heating oil**.

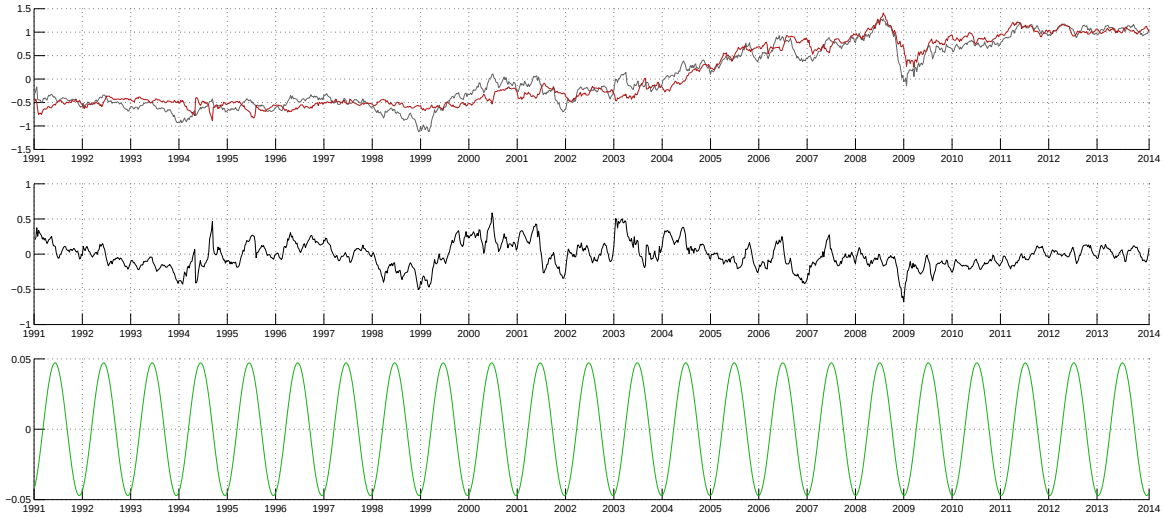

Figure 19. Top panel: Filtered time-series of spot log-prices $\boldsymbol{X}(t)$ (gray line) and long-run log-price level $\boldsymbol{Y}(t)$ (red line) for **gasoline**. **Middle panel:** Differences between short- and long-term log-price levels, i.e., $\boldsymbol{X}(t) - \phi(t) - \boldsymbol{Y}(t)$. **Bottom panel:** Estimated seasonality function for **gasoline**.

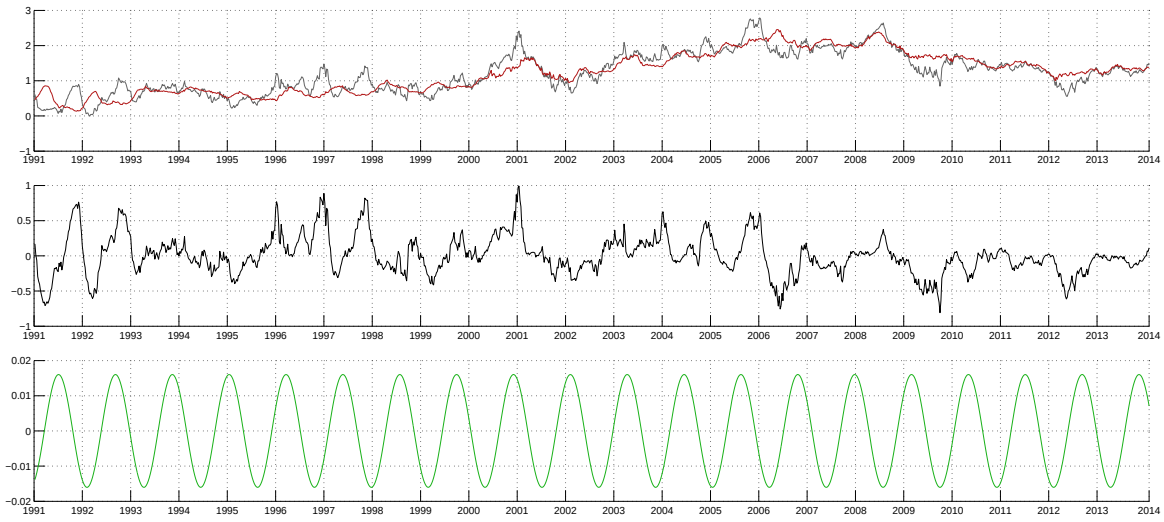

Figure 20. Top panel: Filtered time-series of spot log-prices $\boldsymbol{X}(t)$ (gray line) and long-run log-price level $\boldsymbol{Y}(t)$ (red line) for **natural gas**. **Middle panel:** Differences between short- and long-term log-price levels, i.e., $\boldsymbol{X}(t) - \phi(t) - \boldsymbol{Y}(t)$. **Bottom panel:** Estimated seasonality function for **natural gas**.

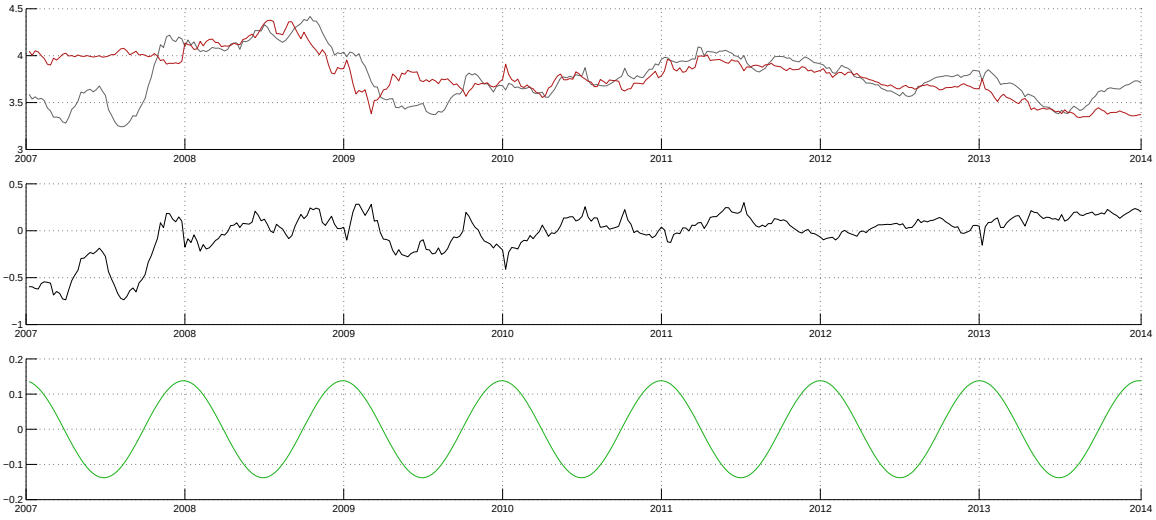

Figure 21. Top panel: Filtered time-series of spot log-prices $\boldsymbol{X}(t)$ (gray line) and long-run log-price level $\boldsymbol{Y}(t)$ (red line) for **power Germany**. **Middle panel:** Differences between short- and long-term log-price levels, i.e., $\boldsymbol{X}(t) - \phi(t) - \boldsymbol{Y}(t)$. **Bottom panel:** Estimated seasonality function for **power Germany**.

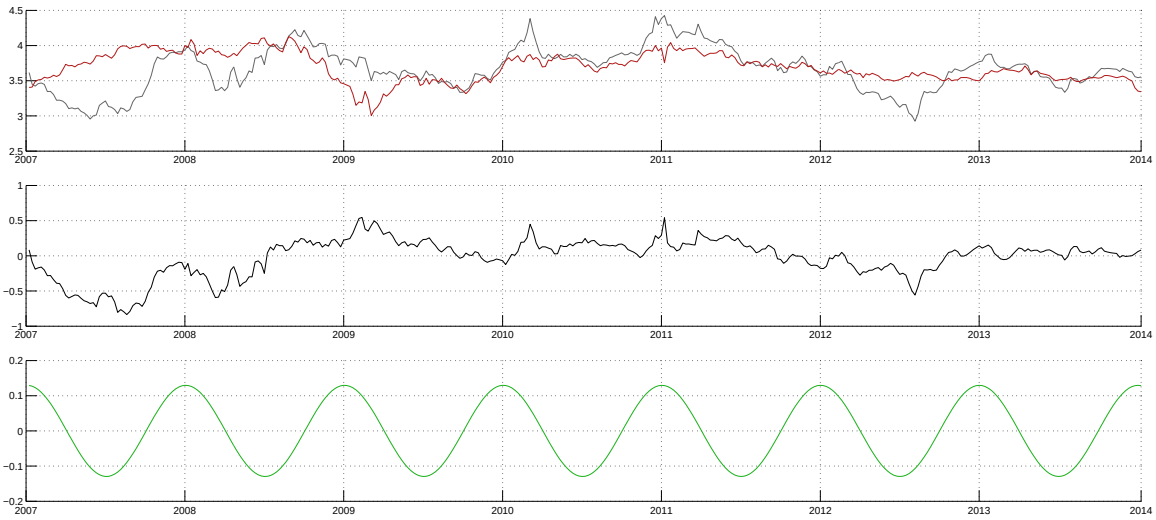

Figure 22. Top panel: Filtered time-series of spot log-prices $\boldsymbol{X}(t)$ (gray line) and long-run log-price level $\boldsymbol{Y}(t)$ (red line) for **power Nordics**. **Middle panel:** Differences between short- and long-term log-price levels, i.e., $\boldsymbol{X}(t) - \phi(t) - \boldsymbol{Y}(t)$. **Bottom panel:** Estimated seasonality function for **power Nordics**.

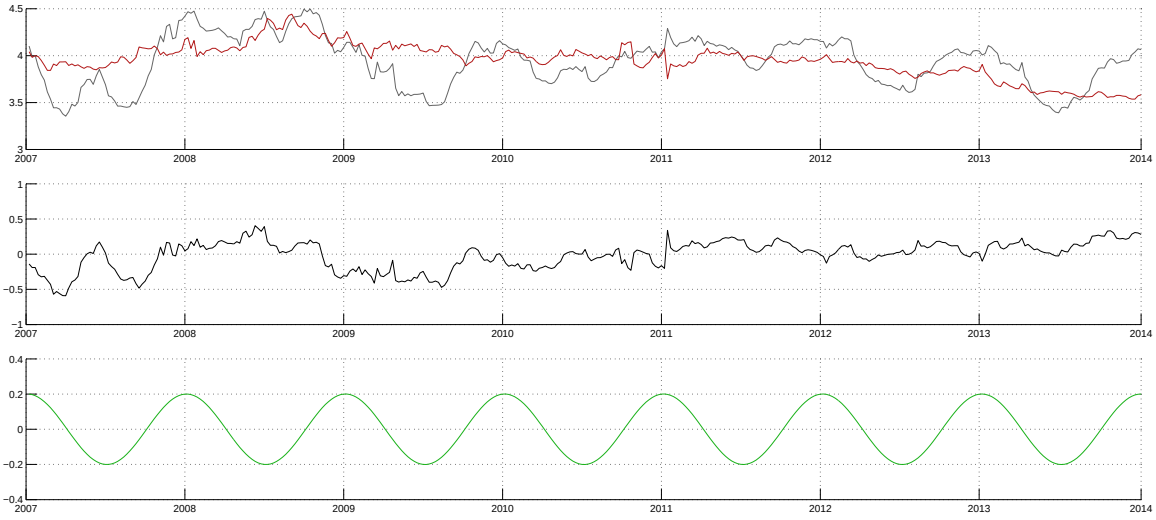

Figure 23. Top panel: Filtered time-series of spot log-prices $\boldsymbol{X}(t)$ (gray line) and long-run log-price level $\boldsymbol{Y}(t)$ (red line) for **power Swiss**. **Middle panel:** Differences between short- and long-term log-price levels, i.e., $\boldsymbol{X}(t) - \phi(t) - \boldsymbol{Y}(t)$. **Bottom panel:** Estimated seasonality function for **power Swiss**.

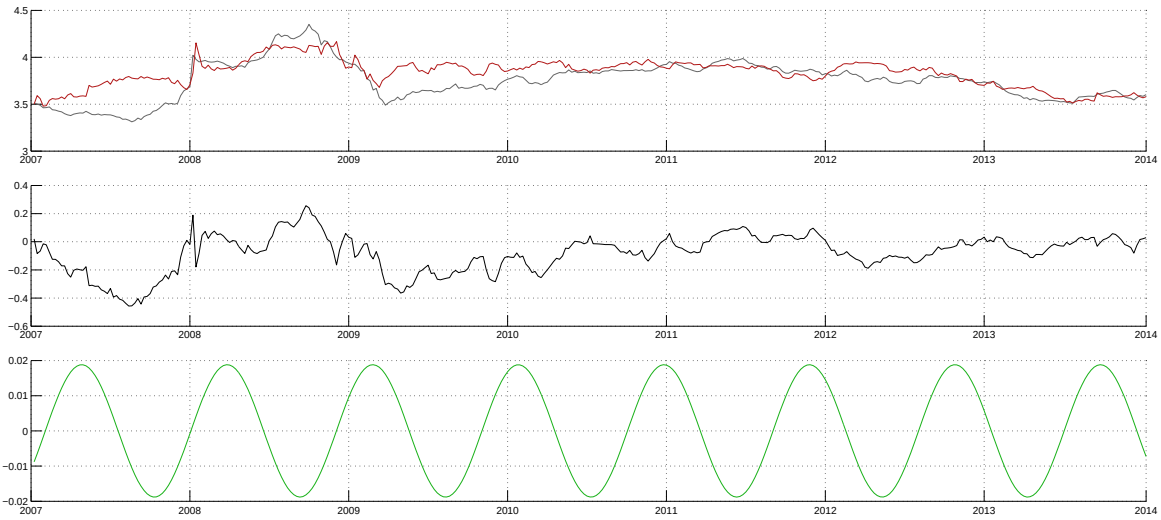

Figure 24. Top panel: Filtered time-series of spot log-prices $\boldsymbol{X}(t)$ (gray line) and long-run log-price level $\boldsymbol{Y}(t)$ (red line) for **power Poland**. **Middle panel:** Differences between short- and long-term log-price levels, i.e., $\boldsymbol{X}(t) - \phi(t) - \boldsymbol{Y}(t)$. **Bottom panel:** Estimated seasonality function for **power Poland**.

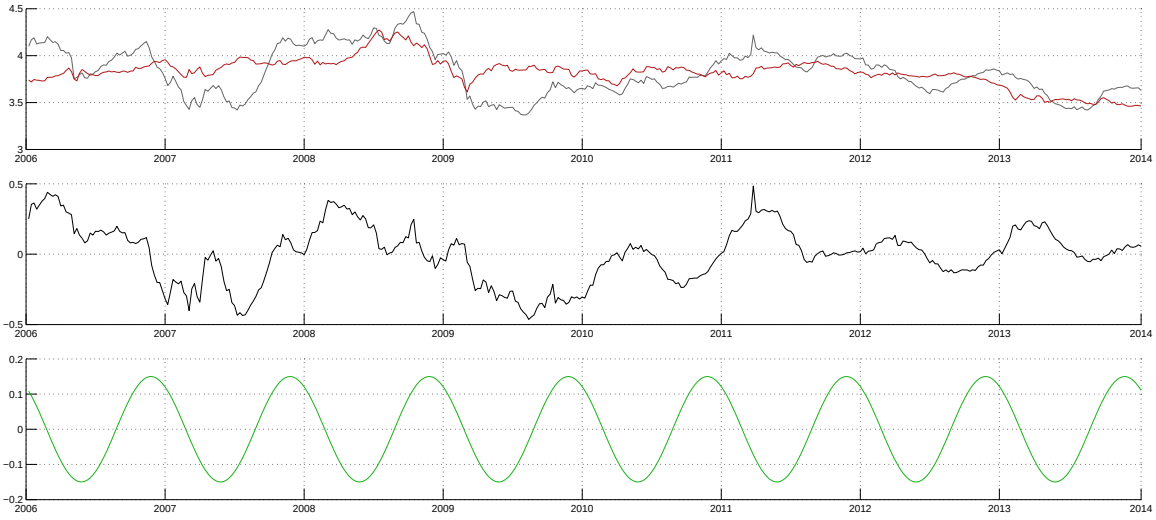

Figure 25. Top panel: Filtered time-series of spot log-prices $\boldsymbol{X}(t)$ (gray line) and long-run log-price level $\boldsymbol{Y}(t)$ (red line) for **electric power** (data set III). **Middle panel:** Differences between short- and long-term log-price levels, i.e., $\boldsymbol{X}(t) - \phi(t) - \boldsymbol{Y}(t)$. **Bottom panel:** Estimated seasonality function for **electric power** (data set III).

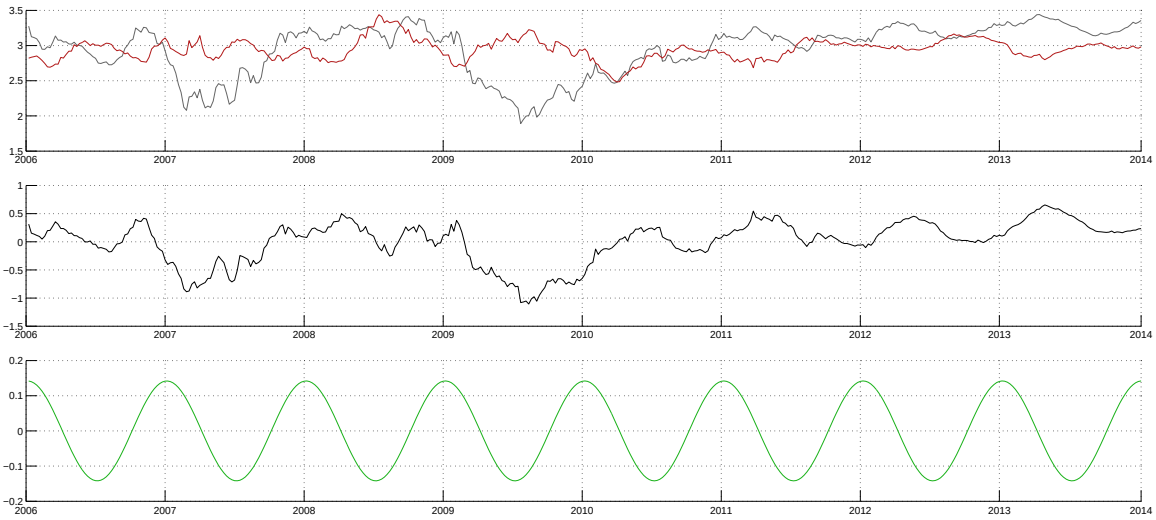

Figure 26. Top panel: Filtered time-series of spot log-prices $\boldsymbol{X}(t)$ (gray line) and long-run log-price level $\boldsymbol{Y}(t)$ (red line) for **natural gas** (data set III). **Middle panel:** Differences between short- and long-term log-price levels, i.e., $\boldsymbol{X}(t) - \phi(t) - \boldsymbol{Y}(t)$. **Bottom panel:** Estimated seasonality function for **natural gas** (data set III).